

UNIVERSITY OF ILLINOIS AT CHICAGO

CME 470

PHYSICAL AND MECHANICAL PROPERTIES OF MATERIALS

---

**Recrystallization Behavior of 70/30 Brass**

---

*Author:*

John KLEIN

*Professor:*

Dr. J.E. INDACOCHEA

**January 12th, 2016**

**UIC** Department of Civil and  
UNIVERSITY OF ILLINOIS  
AT CHICAGO **Materials Engineering**  
COLLEGE OF ENGINEERING

# CONTENTS

<b>I Introduction</b>	<b>1</b>
1.1 Cold working . . . . .	1
1.2 Recovery . . . . .	1
1.3 Recrystallization . . . . .	2
1.4 Grain growth . . . . .	3
1.5 Properties of cartridge brass . . . . .	3
1.6 Recrystallization of cartridge brass . . . . .	4
<b>II Statement of Objectives</b>	<b>5</b>
<b>III Experimental Procedure</b>	<b>5</b>
3.1 Cold work by rolling . . . . .	5
3.2 Annealing . . . . .	6
3.3 Metallography . . . . .	6
<b>IV Results and Discussion</b>	<b>7</b>
4.1 Mechanical properties of cold-rolled cartridge brass . . . . .	7
4.2 Tensile study 1 – recrystallization time . . . . .	9
4.3 Tensile study 2 – recrystallization temperature . . . . .	11
4.4 Effect of annealing on hardness . . . . .	14
4.5 Dependence of recrystallization on anneal time, temperature, and cold work . . . . .	16
<b>V Conclusion</b>	<b>17</b>
<b>References</b>	<b>18</b>
<b>A Appendix</b>	<b>20</b>
A.1 Metallography study 1 – annealing temperature . . . . .	20
A.2 Metallography study 2 – cold work . . . . .	21
A.3 Metallography study 3 – annealing time . . . . .	22
A.4 3D surface (time, % CW, hardness) . . . . .	23

# Recrystallization Behavior of 70/30 Brass

JOHN KLEIN<sup>†</sup>

Cartridge brass undergoes significant changes in mechanical properties as a result of cold work. These changes are effectively reversed in the annealing process returning the metal to its precold-worked state. The major goal of this study is to characterize how the variables of annealing time, temperature, and degree of cold work affect the physical properties of cartridge brass. Tensile tests, hardness tests, and metallographic examination are used in conjunction to assess mechanical and microstructural changes brought on by cold work and annealing. Results indicate that mechanical changes from cold work are more prominent during the first stages of cold work. The time to reach recrystallization is reduced in response to increases in annealing temperature as well as increasing cold deformation. The recrystallization temperature is reduced when time of anneal is increased or degree of cold work is increased. Therefore, recrystallization is driven by strain imposed on the metal during cold working and is a thermally activated process.

## I. INTRODUCTION

COLD deformation and recrystallization of brass are of great industrial importance because of their roles in the fabrication of the metal and because of the dependence of physical properties on the cold working and on the annealing processes that produce recrystallization.<sup>[1]</sup> Changes in the physical properties of metals brought on by cold working such as increases in hardness, yield strength, ultimate strength, coefficient of thermal expansion, and concomitant decreases in ductility, impact strength, formability, and electrical conductivity are reversed by the fundamentally opposing process of annealing.<sup>[2]</sup>

### 1.1. Cold working

When permanent shape change of a metal occurs at temperatures that are low relative to its melting point, it is said to be cold worked. Most of the mechanical energy in this deformation process is converted into heat, but the remainder is stored in the metal, raising its internal energy.<sup>[3]</sup> The stored energy is associated with the movement of a large number of atoms in response to an applied stress, which involves the motion and creation of dislocations. Since each dislocation represents a crystal defect with an associated lattice strain, increasing the dislocation density increases the strain energy of the material.<sup>[4]</sup>

---

<sup>†</sup> JOHN KLEIN, Undergraduate Student studying mechanical engineering at the University of Illinois at Chicago. Contact e-mail: [johnklein1991@gmail.com](mailto:johnklein1991@gmail.com).

*This article replicates experiments performed as early as the 1940's on the grain size refinement of cartridge brass.*

Mutual interactions of dislocations through their strain fields prevent plastic flow—the generation of dislocations and their ability to propagate along close-packed slip planes—from going on indefinitely. The theory of strain hardening states that as a result of plastic deformation there is an enormous increase in the number of dislocations and a corresponding decrease in the ability for the dislocations to move.<sup>[5]</sup>

By increasing the dislocation density, the distance of separation between dislocations decreases. In closer proximity the repulsive effect of dislocation-dislocation strain interactions becomes more pronounced resulting in greater resistance to dislocation motion.<sup>[6]</sup> Dislocations become pinned or tangled. The net effect is that the metal becomes more and more resistant to plastic deformation requiring greater levels of stress to induce any further reduction in area.

### 1.2. Recovery

As a result of the raised free energy, cold-worked metals are unstable, and therefore, tend to revert to a stable state. Increases in temperature (annealing) accelerate the restoration processes of recovery and recrystallization, processes that work to release the free energy in the metal and return it to its stable (annealed) state.<sup>[7]</sup> Three temperature regions distinguish annealing: recovery, recrystallization, and grain growth.

During recovery there is a large reduction in the number of point defects, dislocations of opposite sign attract and annihilate each other, and dislocations rearrange themselves

into lower energy configurations.<sup>[8]</sup> A distinctive feature of the recovery process is that it does not involve any change in the grain structure of the cold-worked metal; the only changes taking place are microscopic rearrangements of atoms within existing grains.

Diffusion increases rapidly with rising temperature and this allows atoms in severely strained regions to move to unstrained positions. The effect is a partial restoration of certain physical properties such as a decrease in hardness, lowering the yield point and tensile strength, increase in ductility, and electrical and thermal conductivities are fully returned to their pre-cold-worked states. Experimentally, the extent of recovery is often measured by the changes in a single material parameter such as hardness, resistivity, or yield stress with respect to time.

In terms of kinetics, for an isothermal anneal the rate of recovery of such a parameter is greatest at the beginning and decreases as a function of time.<sup>[9]</sup> This is because the recovery process occurs more or less homogeneously throughout the material.

For homogeneous reactions the probability for the transformation—i.e. recovery of a material property—to occur is the same for all locations in the virgin system considered.<sup>[10]</sup> As time increases, the transformation rate decreases monotonically from  $t = 0$  onwards. Furthermore, as a process determined by diffusion, the rate of recovery is more rapid as the annealing temperature increases.

### 1.3. Recrystallization

Recrystallization is characterized by the formation of a new set of strain-free equiaxed grains with high angle grain boundaries and low dislocation densities; it is also characterized by the migration of these high angle grain boundaries causing the absorption of point defects and dislocations.<sup>[11]</sup>

New grains form as small nuclei and grow until they completely consume the parent material; these processes involve thermally activated short-range diffusion.<sup>[12]</sup> The observation of new grains in the microstructure is expressed as a fraction or percent recrystallization.

The recrystallization temperature is the temperature where a significant drop in hardness or strength is just detected for a fixed annealing time. Correspondingly, the recrystallization time occurs when a sharp drop in hardness or strength occurs for a fixed annealing temperature.

When modeled as a nucleation and growth phenomenon, controlled by thermally activated processes, whose driv-

ing force is provided by the stored energy of deformation, recrystallization obeys a set of qualitative statements.<sup>[13,14]</sup>

- i. A minimum amount of plastic deformation is needed to initiate recrystallization. The deformation must be sufficient to provide the necessary driving force to sustain growth of a nucleus.
- ii. The recrystallization temperature decreases as the annealing time increases.
- iii. The recrystallization temperature decreases as the strain increases.
- iv. As the amount of plastic deformation increases the size of the recrystallized grain size will be smaller. The number of nuclei or the nucleation rate is more affected by strain than the growth rate. Therefore, a higher strain will provide more nuclei per unit volume and hence a smaller average grain size.<sup>[15]</sup>
- v. For a given amount of deformation the recrystallization temperature will be increased by a larger starting grain size. Because grain boundaries are a favored nucleation site a larger initial grain size provides fewer nucleation sites, the nucleation rate is lowered, and the recrystallization rate is slower or occurs at higher temperatures.
- vi. And finally, for a given amount of deformation, a higher deformation temperature will increase the recrystallization temperature. Deformation at higher temperatures (hot working) generates more recovery during the deformation (dynamic recovery) and the stored energy is lower than a similar amount of strain at a lower deformation temperature.<sup>[16]</sup>

Both recovery and recrystallization are controlled by diffusion of constituent atoms. As such they are temperature and time dependent. Moreover, both processes are driven by the difference in internal energy between the strain-free state and the cold-worked state. Recovery and recrystallization are concurrent processes.

However, there is a clear difference in kinetics between recovery and recrystallization. For an isothermal anneal the reaction rate of recovery is greatest at the onset of annealing. Contrastingly, the reaction rate of recrystallization starts off slowly, builds up to a maximum, and then tapers off as it approaches complete recrystallization.<sup>[17]</sup>

One factor that contributes to the difference in kinetics is that the critical diffusion distance for recovery is less than that of recrystallization.<sup>[18]</sup> The difference in kinetics offers an explanation as to why at lower annealing temperatures and even room temperature the cold worked metal will

spontaneously recover some of its physical properties to the precold-worked state without the formation new grains.

#### 1.4. Grain growth

If a specimen is left at a high temperature beyond the time needed for complete recrystallization, the grains begin to grow in size, a phenomenon termed grain growth. Grain growth is characterized by a coarsening of the microstructure, a reduction in grain boundary area where larger grains grow at the expense of smaller grains, and is driven by the release of grain-boundary energy.<sup>[19]</sup>

Grain growth is distinct from the migration of high-angle grain boundaries in recrystallization in that the driving force for grain growth is smaller and consequently, the velocity of the migrating grain boundaries is slower. In addition, in contrast to recrystallization, the boundary moves towards its center of curvature; some of the grains grow, but others become smaller and vanish.<sup>[21]</sup> With a constant volume, the number of grains decreases during grain growth.

At the grain boundary there are varying degrees of crystallographic misalignment between adjacent grains. As a consequence of the misorientation, atomic bond angles are stretched generating an interfacial or grain-boundary energy. The magnitude of this energy is a function of the degree of misorientation, where high-angle grain boundaries have greater interfacial energy.

Assuming metallic grain growth occurs as a result of interfacial energy considerations and diffusion of atoms across a grain boundary, the kinetics of normal grain growth are modeled in the same form as that of the grain-growth law in soap foam.<sup>[22]</sup> When diffusion is taken as a thermally activated process, the grain-growth law becomes a function of both temperature and time.<sup>[23]</sup> Alternative approaches to model metallic grain growth include a curvature-driven growth model, statistical analysis, stochastic modeling, and numerical simulations.<sup>[24]</sup>

In terms of mechanical properties, all other parameters fixed, fine-grained metals are harder, stronger, and often tougher, than coarse-grained metals. The former has a greater total grain boundary area to impede dislocation motion. The Hall-Petch relationship relates yield strength to the average grain size diameter, where smaller average grain sizes generate higher yield strengths.<sup>[25]</sup>

#### 1.5. Properties of cartridge brass

The alloy of 70% copper and 30% zinc, commonly known as cartridge brass or 70-30 brass is characterized by properties of high strength and ductility, and is capable of deep drawing.<sup>[26]</sup> As indicated in Fig. 1.1, at room temperature cartridge brass is a single-phase ( $\alpha$ -phase) substitutional solid solution of zinc in the FCC copper structure.

Because cartridge brass is a single-phase alloy it is not considered heat treatable, but it can be strengthened by cold working and softened by annealing.<sup>[27]</sup> The high work hardening rate in the alloy means that cold working can increase the yield strength dramatically, from 75 MPa in the fully annealed condition to over 450 MPa in the full-hard condition. Along with the increase in strength, there is a decrease in ductility (% EL) from 68% down to 3%.

Using testing data from the literature, Tables 1.2 and 1.3 demonstrate the changes in mechanical properties of cartridge brass brought on by cold work and annealing. The ASTM standard classifications for temper designations in copper alloys are employed.<sup>[28]</sup> Cold-worked tempers are designated with the letter H and are produced with controlled amounts of area reduction. The annealed tempers designated by OS are tempers produced by annealing to meet standard grain size requirements.

**Table 1.1** General properties of cartridge brass

Properties		
Density (@ 20°C)	8.53 g/cm <sup>3</sup>	
Melting point–liquidus	954°C	
Melting point–solidus	916°C	
Annealing temperature	425–750°C	
Tensile strength (depends on temper)	303–896 MPa	
Yield strength (depends on temper)	75–450 MPa	
Modulus of elasticity	110 GPa	
Poisson's ratio	0.375	
Chemical composition	Element	Content (wt%)
	Cu	68.5–71.5
	Zn	28.5–31.5
	Pb	≤ 0.070
	Fe	≤ 0.015
	Other	≤ 0.15

\*Data is for cartridge brass, UNS C26000 (260 Brass)<sup>[19]</sup>

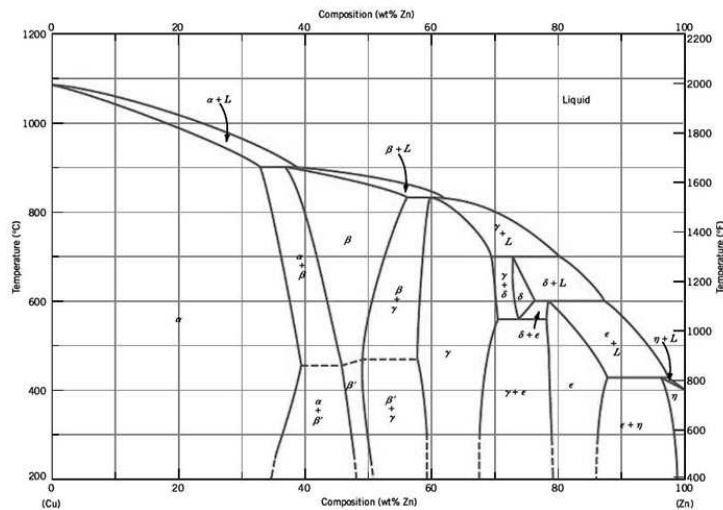


**Fig. 1.1** Copper-zinc phase diagram<sup>[31]</sup>  
 Adaped from *Binary Phase Diagrams*, 2nd Edition, Vol. 2, T.B. Massalski (Editor in Chief), 1990.

**Table 1.2** Effect of cold work on mechanical properties

<b>Cold-worked tempers—H*</b>	H01	H02	H04	H06	H08	H10
Temper name	1/4 Hard	1/2 Hard	Hard	Extra Hard	Spring Hard	Extra Spring
Hardness, Rockwell B	55	70	82	83	91	93
Hardness, Rockwell 30T	54	65	73	76	77	78
Tensile strength, ultimate	370 MPa	425 MPa	525 MPa	595 MPa	650 MPa	680 MPa
Tensile strength, yield	275 MPa	360 MPa	435 MPa	450 MPa	N/A	N/A
Shear strength	250 MPa	275 MPa	305 MPa	315 MPa	330 MPa	N/A
Elongation at break	43%	23%	8.0%	5.0%	3.0%	3.0%

\*Data is for cartridge brass, UNS C26000 (260 brass) H temper flat products — 1mm thickness<sup>[29]</sup>

**Table 1.3** Effect of annealing on mechanical properties

<b>Annealed tempers—OS*</b>	OS015	OS025	OS035	OS050	OS070	OS100
Average grain size	0.015 mm	0.025 mm	0.035 mm	0.050 mm	0.070 mm	0.100 mm
Hardness, Rockwell F	75	72	68	64	58	54
Hardness, Rockwell 30T	43	36	31	26	15	11
Tensile strength, ultimate	365 MPa	350 MPa	340 MPa	325 MPa	315 MPa	300 MPa
Tensile strength, yield	150 MPa	130 MPa	115 MPa	105 MPa	95.0 MPa	75.0 MPa
Shear strength	240 MPa	235 MPa	235 MPa	230 MPa	220 MPa	215 MPa
Elongation at break	54%	55%	57%	65%	65%	68%

\*Data is for cartridge brass, UNS C26000 (260 brass) OS temper flat products — 1mm thickness<sup>[30]</sup>

### 1.6. Recrystallization of cartridge brass

Previous studies on cartridge brass show that during annealing there is a gradual loss in hardness with time, until recrystallization commences. When recrystallization commences, hardness decreases rapidly until complete recrystallization.<sup>[32]</sup> Once recrystallization is complete, any further loss of hardness is due to increased grain size, due to the phenomenon of grain growth.

Importantly, for a given degree of deformation, the hardness number at the point where recrystallization is complete

is constant, regardless of the time and temperature relations necessary to establish complete recrystallization. The hardness number when recrystallization is complete increases with an increase in cold deformation, as a result of the decrease in recrystallized grain size. This observation is explained by recrystallization law (iv), which states that a larger amount of plastic deformation generates more nucleation and a lower average grain size during complete recrystallization.

Separate tests confirm that for a given degree of cold

deformation, the grain size representing complete recrystallization, without appreciable grain growth, is constant and independent of the time and temperature necessary to establish complete recrystallization.<sup>[33]</sup>

For instance, in Walker's landmark study, at 70% cold work and performing annealing to the point of complete recrystallization at temperatures of 350°C, 400°C, 550°C, and 650°C, the average grain diameter was consistently at 0.015 mm.

Moreover, from this 1945 study on cartridge brass, a higher annealing temperature required less time to produce complete recrystallization for a constant degree of cold deformation—i.e., the results obeyed recrystallization law (ii). To give an example, the time to reach complete recrystallization at 650°C with 42% CW only took 15 seconds whereas for the same amount of deformation at 450°C it took 16 minutes to reach complete recrystallization.

In accordance with recrystallization law (iii)—which states that increased strain on the metal decreases the annealing temperature—the time to reach complete recrystallization at 450°C 21% CW was 4 hours whereas at 42% CW at the same annealing temperature it only took 15 seconds to reach complete recrystallization.

## II. STATEMENT OF OBJECTIVES

The purpose of this experiment is, first, to examine how the independent variables of:

1. % CW
2. time of anneal
3. temperature of anneal

affect the physical properties of cartridge brass. Second, from this data determine the time to recrystallization at each annealing temperature as well as the recrystallization temperature for different annealing times. The degree of cold work is considered in how it affects the times and temperatures of recrystallization.

Physical properties under investigation are principally:

- hardness  $(R_B)$
- yield strength  $(\sigma_y)$
- ultimate tensile strength  $(\sigma_{TS})$
- percent elongation  $(\% EL)$
- microstructure

The means to obtain these properties are through Rockwell hardness testing machines, tensile tests, and metallographic inspection.

Several analytical techniques are implemented in order to assess how the independent variables affect material properties. Hardness values and tensile test properties including: yield strength, tensile strength, and percent elongation are plotted when 1 of the 3 independent variables

is varied, such as degree of deformation while keeping the other 2 fixed, such as annealing time and temperature. Graphs may incorporate multiple sets of data so as to investigate how the variables work in relation to each other.

From these plots, the temperature where a significant drop in hardness or strength or significant increase in ductility is *just* detected for a fixed time is the recrystallization start temperature. Similarly, the time at which a significant drop in hardness or strength or significant increase in ductility is *just* detected for a fixed recrystallization temperature is declared the start time of recrystallization.

Finally, because of the inextricable link between microstructure and mechanical properties, metallographic examination is used to support the results obtained in the plots. Metallography depicts the underlying microstructural phenomena such as elongation of grains and an increase in grain boundary through cold work. Metallography is used to demonstrate microstructural changes during the stages of annealing—i.e., it depicts characteristic changes during recovery, recrystallization, and grain growth.

## III. EXPERIMENTAL PROCEDURE

### 3.1. Cold work by rolling

Ten brass strips of dimensions 1"×1/8"×6" are acquired in an annealed condition. Rockwell B scale hardness numbers are obtained for the starting material using a Wilson Tester model 3JR set to a 100 kgf major load with a 1/16" diameter diamond ball indenter. In addition, a 30 kgf load is applied using the same indenter generating Rockwell 30T hardness numbers. To achieve statistical significance at least 3 measurements are taken and the average is computed.

The brass strip sections are then cold rolled to each of the following area reductions: 0%, 25%, 50%, and 75%. The initial thickness of the sections was measured to be on average 3.2 mm. To obtain a 25%, 50%, and 75% reduction in area, sections are cold rolled to a final thickness of 2.4 mm, 1.6 mm, and 0.8 mm, respectively.

In total, 2 samples are left in the annealed (0% CW) state, 2 are cold rolled to 25% CW, 3 are cold rolled to 50% CW, and 3 are rolled to 75% CW. Hardness  $R_B$  and 30T values are measured for the cold rolled specimens.

A 6" sample is cut from each brass section and five additional 6" samples are cut for the 50% and 75% cold rolled specimens. The 6" cuts are then machined into the dimensions as specified by the ASTM E8 Standard Tensile Specimen (width: 0.250±0.005", gage length: 1.000±0.003", radius of fillet: 0.250", overall length: 4.000", length of reduced section 1.250", length of grip section: 1.250", width of grip section ≈ 0.375").<sup>[34]</sup>

### 3.2. Annealing

Approximately 20 coupons are cut and labeled from each rolled strip. Four specimens, one from each degree of cold work (0%, 25%, 50%, and 75%) are placed in a single packet. The packets are subjected to the heat treatments according to Table 3.1. Only those treatments marked with a check mark are performed.

There are 20 different treatments for a total of 80 annealed specimens. Additionally, one set of samples (one packet) is to remain in the as-rolled condition. As the coupons are removed from the furnace, they are water quenched. The samples are cleaned using an abrasive paper and the  $R_B$  and 30T hardness numbers are measured.

In addition to annealing the coupons, four 75% CW tensile specimens are annealed for 5 minutes at 100°C, 300°C, 425°C, and 550°C and five 50% CW tensile specimens are annealed at 425°C for 2, 5, 10, 30, and 60 minutes.

Tensile tests are conducted on the nine annealed tensile specimens and on four specimens that did not receive any heat treatment at each degree of cold work (0%, 25%, 50%, 75%). Tensile tests are performed using the Instron Tensile Tester model number 5500R at a strain rate of 0.5"/min. The machine conforms to the requirements of ASTM Practices E4 in that the forces used in determining tensile and yield strengths are within the verified force applications of the machine.

The properly machined specimen in the wedge grips of the testing machine ensures that the specimen under load shall be as nearly as possible in uniformly distributed pure axial tension.<sup>[35]</sup> An extensometer is used to measure the strains associated with the stress exerted on the specimen throughout the tensile test and conforms to the requirements of ASTM Practices E83.

### 3.3. Metallography

Based on the hardness and tensile test results, three sets of coupons are chosen to be metallographically examined:

1. The first set includes four coupons that were all annealed for 30 minutes at 75% CW where only *the annealing temperature is varied* (100°C, 300°C, 425°C, and 550°C).
2. The second set includes four coupons all annealed at 425°C for 1 hour where only *the percentage cold work is varied* (0%, 25%, 50%, 75%).
3. The third set consists of four coupons all with 50% CW and annealed at 550°C where only *the annealing time is varied* (2 min, 5 min, 30 min, 1 hour).

The ASTM E3 standard is implemented in order to prepare the three sets of coupons to be observed under a light microscope. Each set (4 samples) is hot mounted on a 1.25"

diameter disc using a 2-part system consisting of 10 parts by weight epoxy resin and 1 part by weight catalyst.

Coarse grinding is performed in order to planarize the mount surface. Using successively finer abrasives papers, fine grinding is performed. Manual polishing is then carried out using a 10  $\mu$ m alumina powder embedded in water.

At this point, the mounts are etched with 1 part nitric acid and 1 part distilled water. Upon successful exposure to the etchant the microstructure is examined using a light microscope. The specimens are photographed at 200X and 500X magnifications.

**Table 3.1** Heat treatments

Time	Temperature			
	100°C	300°C	425°C	550°C
2 min			✓	✓
5 min	✓	✓	✓	✓
10 min			✓	✓
30 min	✓	✓	✓	✓
60 min			✓	✓
150 min	✓	✓		
24 hours	✓	✓		
1 week	✓	✓		

## IV. RESULTS AND DISCUSSION

### 4.1. Mechanical properties of cold-rolled cartridge brass

In Fig. 4.1 (a), the percentage cold deformation is plotted against the Rockwell B hardness. Hardness goes up rapidly during the initial stages of cold work—e.g., from 0% CW to 25% CW hardness increases 52  $R_B$  numbers. Thereafter, the increase in Rockwell B hardness slows. There is only a 9.7  $R_B$  increase when deformation is further increased from 25% to 75%. The regression curve depicts how  $R_B$  rises abruptly at low levels of deformation and then levels out approaching a maximum.

% CW	$R_B$	$\sigma_y$ (MPa)	$\sigma_{TS}$ (MPa)	% EL
0	27.5	193	269	35
25	79.5	360	425	27
50	86.8	462	505	21
75	89.2	524	563	12

**Table 4.1** Physical properties of cold-rolled cartridge brass. Data are used in Fig. 4.1 and represent averages taken over multiple brass sections ( $R_B$ ) and tensile specimens ( $\sigma_y$ ,  $\sigma_{TS}$ , % EL) at each level of cold work.

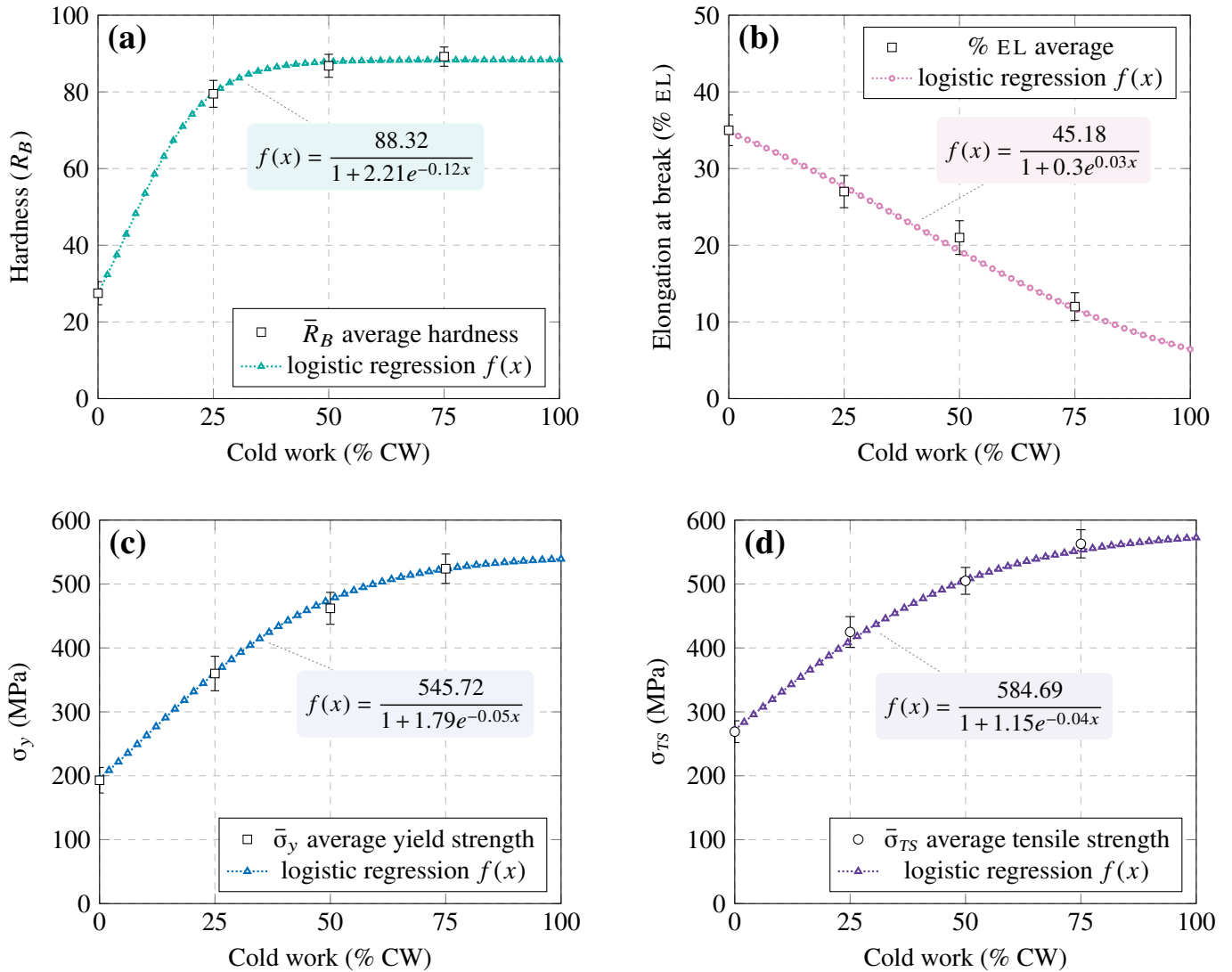


**Fig. 4.1** Hardness test and tensile test properties of cold-rolled cartridge brass. (a): Hardness ( $R_B$  / Rockwell B) test results obtained from rolled brass sections. (b): Percent elongation % EL results obtained from tensile specimens. (c): Yield strength  $\sigma_y$  results derived from tensile specimens. (d): Ultimate tensile strength  $\sigma_{TS}$  results derived from tensile specimens. Error bars indicate a 95% confidence interval. For each graph a logistic regression curve is developed.

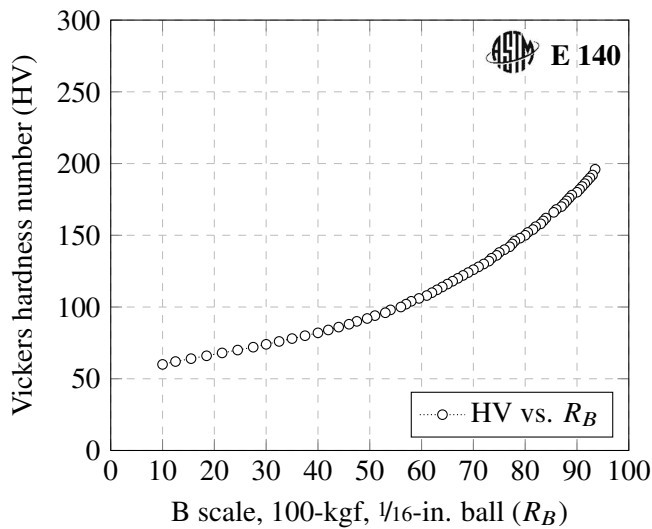


**Fig. 4.2** Approximate hardness conversion numbers for cartridge brass (70% copper 30% zinc alloy). Rockwell and Vickers data are taken from ASTM E 140 and plotted as white circles.

A hardness of 100  $R_B$  is defined as zero penetration. Decrementing by one Rockwell number represents an indentation of 0.002 mm. Because the Rockwell B scale is defined so that zero penetration means 100  $R_B$ , an infinitely hard material would have a finite hardness of 100  $R_B$ . In other words, Rockwell hardness is non-linear, especially when approaching the maximum 100  $R_B$ . Suffice to say, a 100  $R_B$  is not twice as hard as a 50  $R_B$ .

In Fig. 4.2, the Vickers hardness number (HV) is plotted against Rockwell B hardness using data from ASTM E 140. The advantage of Vickers hardness (also known as diamond pyramid hardness DPH), is that it is a linear scale—infinately hard materials would have an infinite HV—and, moreover, it is empirically proportional to the compressive strength of the material.

A quick glance at the conversion graph shows  $R_B$  hardness is not linearly related to Vickers hardness. The slope of HV vs.  $R_B$  increases approaching 100  $R_B$ . The increase in HV required to go from 70  $R_B$  to 80  $R_B$  is less than that required to go from 80 to 90  $R_B$ .

The equivalent HV values at each level of cold work in Table 4.2 are graphed in Fig. 4.3. The change in equivalent Vickers hardness is not as dramatic as the change in Rock-

% CW	$R_B$	Indentation depth	Equivalent Vickers hardness
0	27.5	0.0145 mm	72 HV
25	79.5	0.0041 mm	149 HV
50	86.8	0.0026 mm	169 HV
75	89.2	0.0022 mm	178 HV

**Table 4.2** Hardness data where indentation depth is calculated as  $(100 - R_B) \times 0.002$  mm. Equivalent Vickers hardness is determined using the hardness conversion chart, Fig. 4.2.

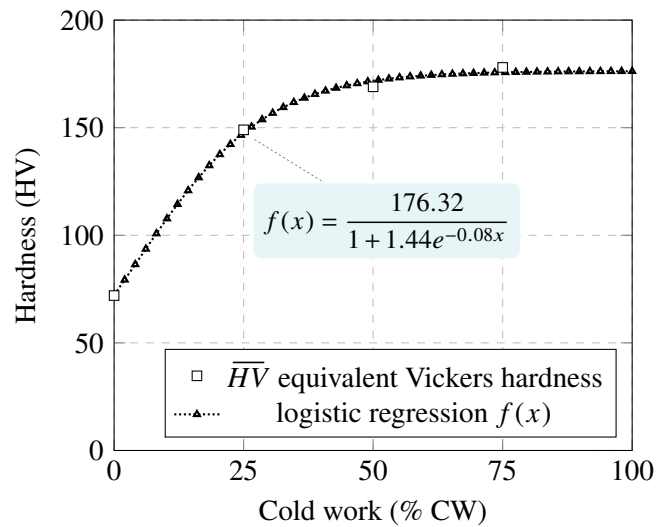


**Fig. 4.3** Equivalent Vickers micro hardness as a function of cold work. Fig. 4.1 (a) is re-graphed in terms of HV, which is converted from  $R_B$  using ASTM E 140.

well B hardness. However, the general trend is the same. Going from 0% to 25% CW, there is a 77 HV increase, while going from 25% to 75% CW there is only a 29 HV increase.

The Vickers graph above reaffirms earlier conclusions based off the  $R_B$  data. Hardness data support the theory of strain hardening. The material is more amenable to hardening during the first stages of cold working. By 25% CW the rate at which the hardness increases drops off significantly, meaning that any further reduction in area gives diminishing returns in terms of hardness.

As shown in Fig. 4.1 (b), the percent cold work is plotted against percent elongation % EL. Percent elongation is taken to be the strain at the point of rupture during the tensile test. The trend observed is a more or less constant linear decrease in % EL as the amount of cold work done increases. On average, there is a 23% decrease in elongation from the annealed/as received state to the 75% cold worked specimen.

In Fig. 4.1 (c) the percentage cold deformation is plotted against the yield strength  $\sigma_y$ . Similar to the pattern observed in regards to hardness although less pronounced, the yield strength rises more quickly at the initial stages of cold work and gradually levels off. The increase in yield strength amounts to 167 MPa when the deformation is increased from 0% to 25% CW. Thereafter, the increase slows down, amounting to an almost equal amount of 164 MPa when the area is further reduced from 25% to 75%. The regression curve depicts how the yield strength rises with increased cold work, albeit at marginally lower and lower rates.

In Fig. 4.1 (d), the percentage cold work is plotted against the ultimate tensile strength  $\sigma_{TS}$ . The dependences

## 4.2. Tensile study 1 – recrystallization time

**Table 4.3** Summary of tensile study 1

Independent variable	Controls	Dependent variables <sup>a</sup>
Annealing time	Annealing temperature: 425°C Cold work: 50% CW Strain rate: 0.5/min <sup>b</sup>	$\sigma_y$ $\sigma_{TS}$ % EL $E^c$

<sup>a</sup> The dependent variables or outputs are the mechanical properties derived from the tensile test.

<sup>b</sup> For a strain rate of 0.5 per minute and a specimen gage length of 1", where Strain rate  $\times$  Gage length = Position rate, the Position rate of the crossheads—i.e., speed that tensile specimen is being pulled apart, is 0.5" per minute.

<sup>c</sup> Young's modulus is denoted by  $E$ .

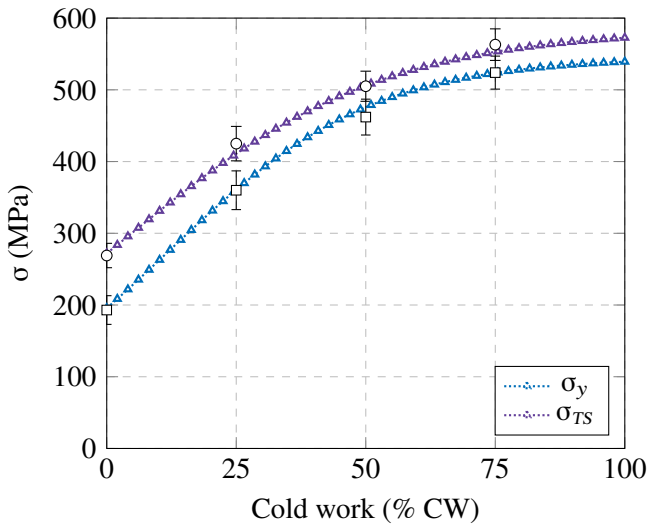


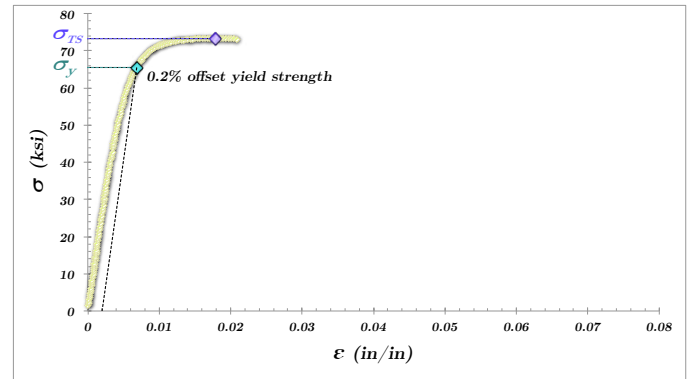
**Fig. 4.4** Ultimate tensile strength and yield strength as a function of cold work in rolled cartridge brass. Graphs (c) and (d) from Fig. 4.1 are plotted on the same axes. Although both  $\sigma_y$  and  $\sigma_{TS}$  increase as the material is cold worked, the gap between the two properties narrows. Yield strength is more greatly affected by cold work than ultimate tensile strength. The yield strength increases 37 MPa more than the tensile strength going from 0% to 75% CW.

of  $\sigma_y$  and  $\sigma_{TS}$  on % CW are comparable. The increase in tensile strength amounts to 156 MPa when the deformation is increased from 0% to 25% CW. Thereafter, the increase slows, amounting to only 138 MPa when the area is further reduced from 25% to 75% CW. The trend line shows how  $\sigma_{TS}$  rises with increased cold work albeit at marginally lower and lower rates.

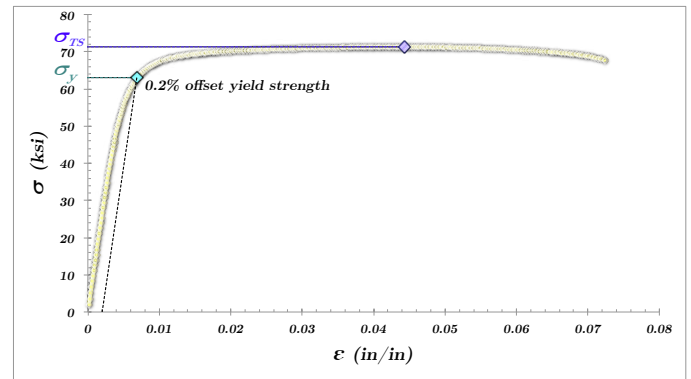
As shown in Fig. 4.4, which plots  $\sigma_{TS}$  and  $\sigma_y$  as a function of % CW on the same axes, increases in cold deformation have a somewhat greater effect on the magnitude of the yield strength compared to the magnitude of the ultimate tensile strength. The gap between  $\sigma_y$  and  $\sigma_{TS}$  shortens with increasing cold deformation;  $\sigma_y$  increases at a greater rate.

To put in perspective the mechanical changes caused by cold working brass to a 75% area reduction, compared to the initial value of the property in the precold-worked state there was:

- over a 200% increase in  $R_B$  hardness,
- a 147% increase in equivalent HV hardness,
- over a 200% increase in yield strength,
- over a 100% increase in ultimate tensile strength, and
- a 23% decrease in ductility—% EL.



(a) 50% CW, no annealing



(b) 50% CW, annealed for 2 minutes at 425°C

**Fig. 4.5** Stress-strain graphs of cartridge brass tensile specimens cold rolled to 50% CW. After 2 minutes of annealing at 425°C there is slight restoration mechanical properties, which is characteristic of the recovery stage.  $\sigma_{TS}$  and  $\sigma_y$  remain relatively high. The strain  $\epsilon$  at fracture remains low. Recrystallization is likely just beginning.

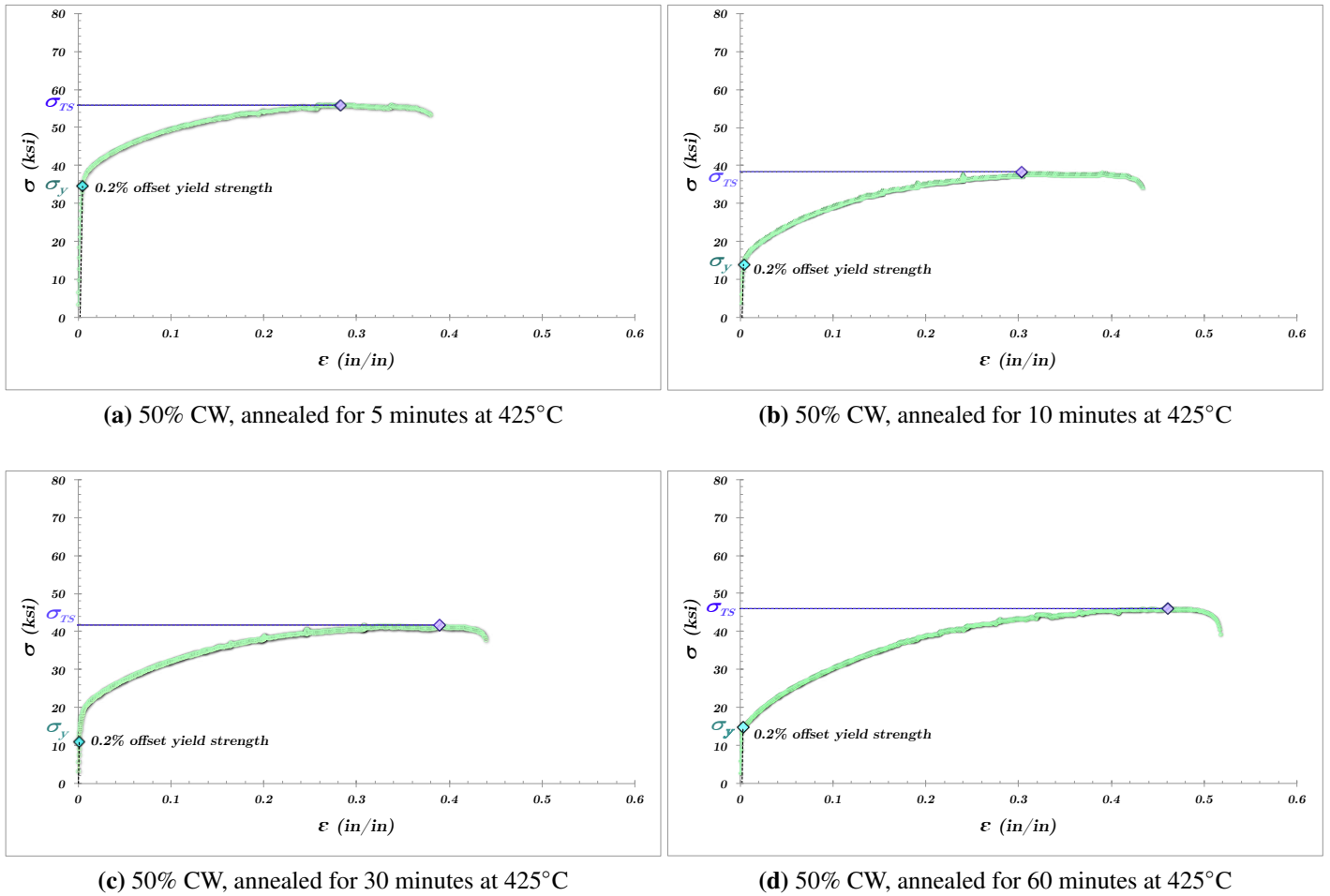


**Fig. 4.6** Stress-strain graphs (cont.). Results of cartridge brass tensile specimens cold-rolled to 50% CW annealed for 5, 10, 30, and 60 minute times at a temperature of 425°C. Significant restoration of mechanical properties is well underway by the 5 minute mark. Note that the dimensionless strains  $\epsilon$  at fracture in these graphs are significantly greater compared to  $\epsilon$  at fracture in the previous two graphs in Fig. 4.5 (a) and (b).

**Table 4.4** Mechanical properties

50% CW, 425°C anneal

Time	0 min	2 min	5 min	10 min	30 min	60 min	0 min	2 min	5 min	10 min	30 min	60 min
$\sigma_{TS}$	505 MPa	492 MPa	386 MPa	265 MPa	290 MPa	317 MPa	73 ksi	71 ksi	56 ksi	38 ksi	42 ksi	46 ksi
$\sigma_{y-0.2\% \text{ offset}}$	462 MPa	434 MPa	241 MPa	97 MPa	76 MPa	103 MPa	67 ksi	63 ksi	35 ksi	14 ksi	11 ksi	15 ksi
$E$	93 GPa	90 GPa	88 GPa	64 GPa	88 GPa	103 GPa	13,500 ksi	13,000 ksi	12,816 ksi	9,302 ksi	12,816 ksi	14,952 ksi
% EL	2.1%	7.2%	38%	43%	44%	52%						

(a) SI units

(b) Imperial units

Properties obtained from stress-strain graphs of cold-rolled cartridge brass, 50% CW and annealed for variable time at 425°C. Significant changes in  $\sigma_{TS}$ ,  $\sigma_y$ , and % EL occur between 2 and 5 minutes. At this level of cold work and at this annealing temperature, the time to reach recrystallization is around 2 minutes.

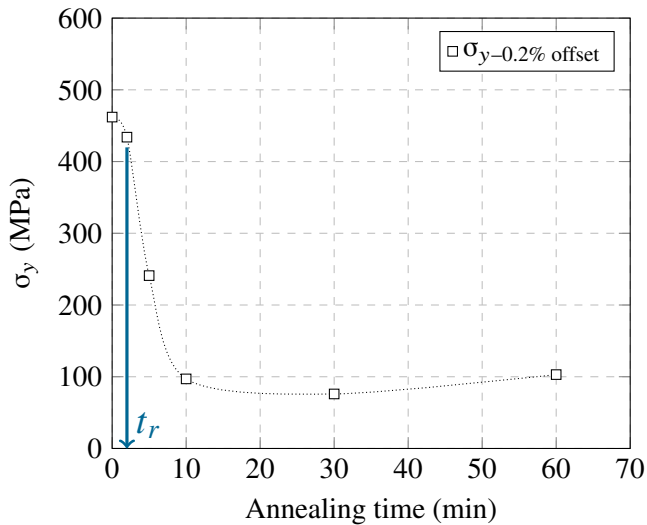


**Fig. 4.7** Yield strength  $\sigma_{y-0.2\% \text{ offset}}$  for cartridge brass cold rolled to 50% CW and annealed for variable time at 425°C. The start time of recrystallization  $t_r$  is defined as the point where a steep drop in  $\sigma_y$  is just detected, which is about 2 minutes.

Recrystallization starts around 2 minutes. At this time there begins a significant decrease in  $\sigma_y$  and  $\sigma_{TS}$  and an increase in % EL. By 10 minutes, the rate of restoration of properties levels out. Fig. 2 (c) in *Metallography study 2, section A.2* reveals a 50% CW specimen in a late stage of recrystallization at the 60-minute mark. The grain size is still fine compared to the 0% CW specimen in Fig. 2 (a) indicating that recrystallization is not yet complete even at the 60-minute mark. So while mechanical properties more or less stabilize by 10 minutes, the grain structure is not fully restored after 60 minutes of annealing at 425°C.

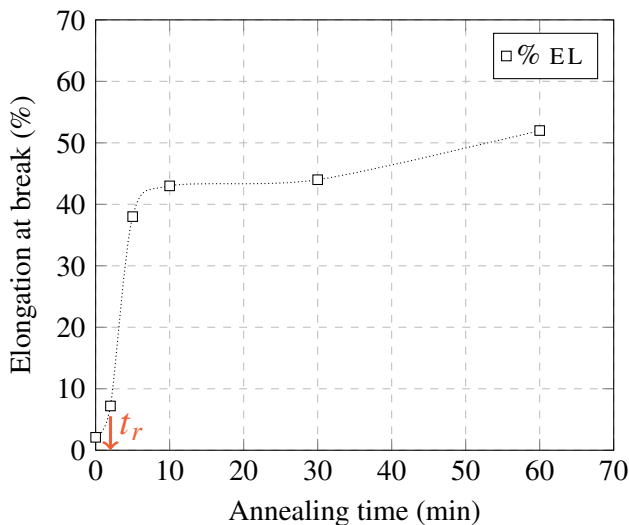


**Fig. 4.8** Elongation at fracture % EL for cartridge brass cold rolled to 50% CW and annealed for variable time at 425°C. The time to reach recrystallization  $t_r$  is defined as the point where a steep increase in % EL is just detected.

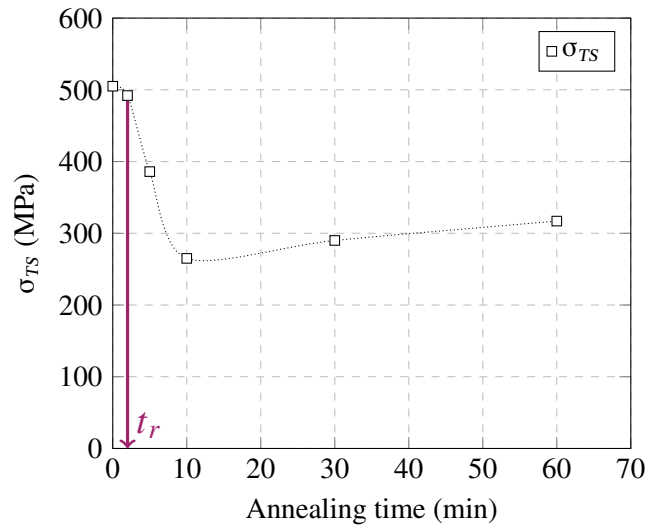


**Fig. 4.9** Ultimate tensile strength  $\sigma_{TS}$  for cartridge brass cold rolled to 50% CW and annealed for variable time at 425°C. The time to reach recrystallization  $t_r$  is defined as the point where a steep drop in ultimate strength is first detected.

The fluctuation of  $\sigma_y$  and  $\sigma_{TS}$  at the times of 10, 30, and 60 minutes, and the variation of  $E$  across all trials are a product of the range of compositions, material processing, and uncertainties in the tensile test. More tests would demonstrate a normal distribution of mechanical properties at each time interval.

Theoretically, with prolonged annealing a continued increase in grain diameter would decrease the yield strength. In a larger grain more dislocations pile up at the boundary. The result is a lower applied stress produces a local stress great enough to cause the grain boundary to collapse. Thus, it is expected that with more trials  $\sigma_y$  at 60 minutes would on average be lower than  $\sigma_y$  at 30 minutes.

From Fig. 4.7, 4.8, and 4.9, the graphs of properties obtained from the stress-strain graphs, there is a more significant restoration of  $\sigma_y$  compared to  $\sigma_{TS}$ . After 10 minutes of annealing at 425°C,  $\sigma_y$  went from 462 to 97 MPa (a 79% decrease) while  $\sigma_{TS}$  went from 505 to 265 MPa (a 47% decrease). At the 10 minute mark, % EL increased by 40.9% (from 2.1% to 43%) effectively restoring ductility to the pre-cold-worked state.

### 4.3. Tensile study 2 – recrystallization temperature

**Table 4.5** Summary of tensile study 2

Independent variable	Controls	Dependent variables
Annealing temperature	Annealing time: 5 minutes Cold work: 75% CW Strain rate: 0.5/min	$\sigma_y$ $\sigma_{TS}$ % EL $E$

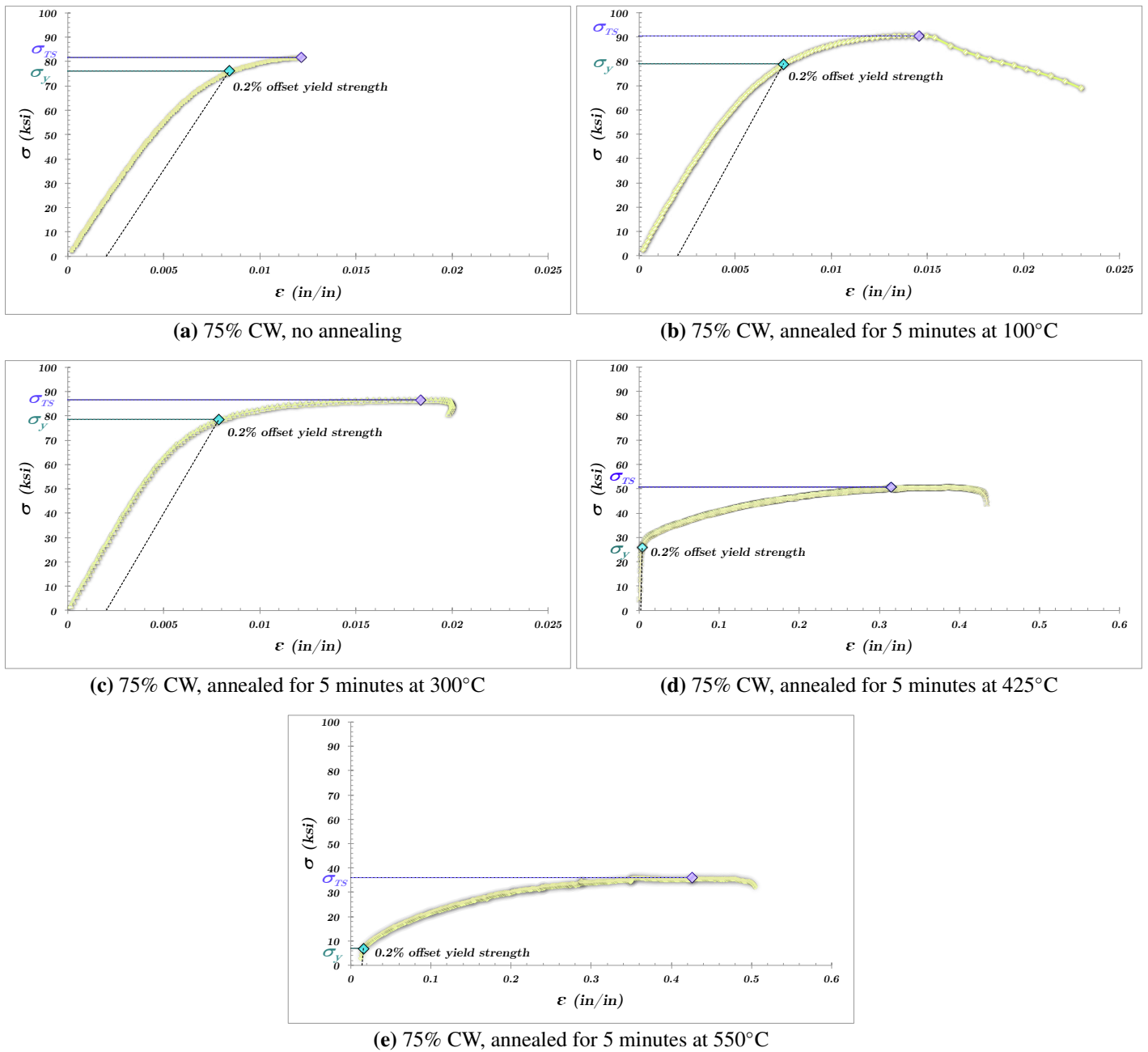


**Fig. 4.10** Stress-strain test results of cartridge brass tensile specimens cold-rolled to 75% CW and annealed for 5 minutes at temperatures of 100, 300, 425, and 550°C. Significant restoration of mechanical properties occurs between 300 and 425°C. Note that the dimensionless strains  $\epsilon$  at fracture at 425°C (d) and 550°C (e) are significantly greater compared to  $\epsilon$  at fracture for the non-annealed (a), 100°C (b), and 300°C (c) specimens.

**Table 4.6** Mechanical properties

Temperature	75% CW, 5 minute anneal									
	No annealing (23°C)	100°C	300°C	425°C	550°C					
$\sigma_{TS}$	563 MPa	623 MPa	597 MPa	352 MPa	248 MPa	82 ksi	90 ksi	87 ksi	51 ksi	36 ksi
$\sigma_{y-0.2\% \text{ offset}}$	524 MPa	545 MPa	544 MPa	179 MPa	48 MPa	76 ksi	79 ksi	79 ksi	26 ksi	7 ksi
$E$	82 GPa	99 GPa	93 GPa	98 GPa	27 GPa	11,900 ksi	14,343 ksi	13,400 ksi	14,250 ksi	3,883 ksi
% EL	1.2%	2.3%	2.1%	44%	50%					

(a) SI units

(b) Imperial units

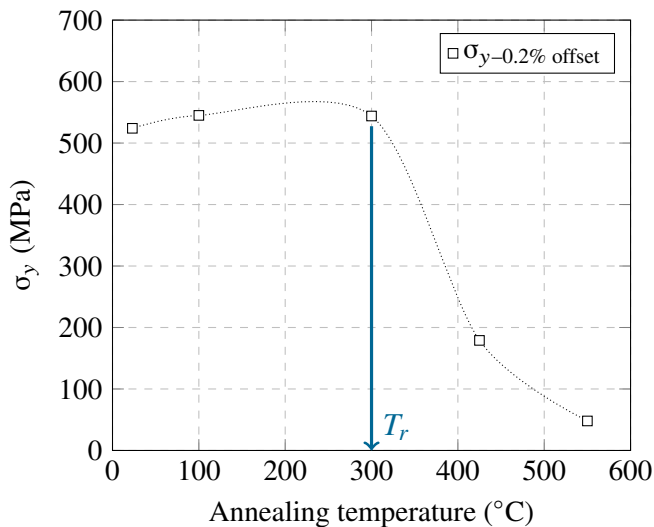


**Fig. 4.11** Yield strength  $\sigma_{y-0.2\% \text{ offset}}$  for cartridge brass cold rolled to 75% CW and annealed for 5 minutes at variable temperature. The recrystallization start temperature  $T_r$  is defined as the point where a steep drop in  $\sigma_y$  is first detected.

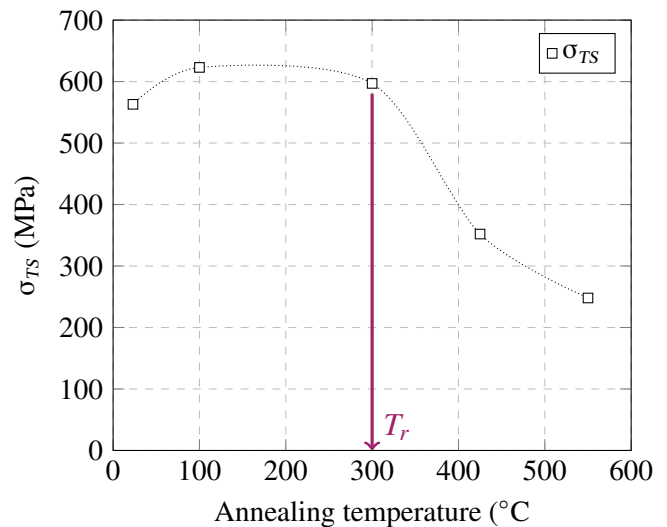


**Fig. 4.13** Ultimate tensile strength  $\sigma_{TS}$  for cartridge brass cold rolled to 75% CW and annealed for 5 minutes at variable temperature. The recrystallization start temperature  $T_r$  is defined as the point where a steep drop in ultimate strength is *just* detected.

Properties derived from tensile data ( $\sigma_y$ ,  $\sigma_{TS}$ , and % EL) are tabulated in Table 4.6 and graphed as a function of annealing temperature in Fig. 4.11, 4.12, and 4.13. The recrystallization start temperature  $T_r$ —defined as the temperature where steep changes in mechanical properties are *just* detected—occurs at approximately 300 $^{\circ}\text{C}$  when 75% CW cartridge brass is annealed for a time of 5 minutes. Yield strength, ultimate strength, and elongation data all converge to  $T_r = 300^{\circ}\text{C}$ . The high degree of plastic deformation is the driving force for recrystallization and the reason

why it occurs at a relatively low annealing temperature.

Similar to the previous tensile study where annealing time is increased at a constant annealing temperature, when annealing temperature is increased at a constant annealing time there is a more dramatic effect in the change in the yield strength  $\sigma_{y-0.2\% \text{ offset}}$  compared the ultimate strength  $\sigma_{TS}$ . This again leads to the conclusion that the physical changes brought on by cold work are being restored to the precold-worked state through the annealing process.

At high degrees of cold work,  $\sigma_y$  and  $\sigma_{TS}$  are nearer to each other. With increasing time or temperature of anneal, the difference between  $\sigma_y$  and  $\sigma_{TS}$  widens as they drop in magnitude. In other words, annealing has a greater impact on 70/30 brass' tendency to yield compared to its tendency to fracture.

At an annealing temperature of 550 $^{\circ}\text{C}$ ,  $\sigma_y$  and  $\sigma_{TS}$  fall below the as-received (0% CW) condition while % EL is well above the as-received condition. Recrystallization is likely coming to an end. In *Metallography study 1, section A.1* Fig. 1 (d), the 75% CW microstructure is shown at 30 minutes time and 550 $^{\circ}\text{C}$  annealing temperature. The microstructure is extremely coarse. The grain growth process may begin as early as 5 minutes in light of the aforementioned stress-strain results.

Glancing at Fig. 4.11, 4.12, and 4.13, the rates of change of a mechanical property ( $\sigma_y$ ,  $\sigma_{TS}$ , and % EL) as a function of annealing temperature begin to level out past 425 $^{\circ}\text{C}$ . This lends to the notion that recrystallization is completed when brass specimens are annealed for 5 minutes at a temperature around 425–550 $^{\circ}\text{C}$ .

Comparing stress-strain properties obtained for the 75% CW sample annealed for 5 minutes at 425 $^{\circ}\text{C}$  in this study

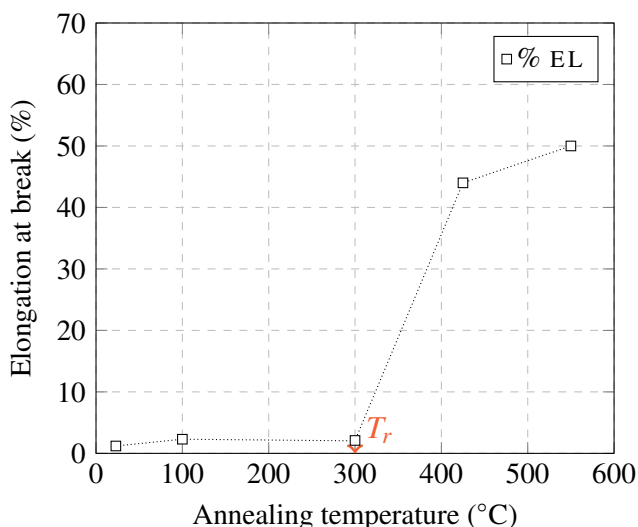


**Fig. 4.12** Elongation at fracture % EL for cartridge brass cold rolled to 75% CW and annealed for 5 minutes at variable temperature. The recrystallization start temperature  $T_r$  is defined as the point where a steep increase in % EL is *just* detected.

vs. the 50% CW sample annealed for the same time and temperature in the previous study, a larger amount of initial cold deformation results in lower  $\sigma_y$  and  $\sigma_{TS}$  and higher % EL. This is shown below:

- 75% CW annealed for 5 minutes at 425°C:
  - $\sigma_{TS}$  = 352 MPa
  - $\sigma_y$  = 179 MPa
  - % EL = 44 %
- 50% CW annealed for 5 minutes at 425°C:
  - $\sigma_{TS}$  = 386 MPa
  - $\sigma_y$  = 241 MPa
  - % EL = 38 %

The initial strain on the material is the driving force for heat-induced recrystallization and restoration of material properties to the precold-worked state. Assuming there is sufficient heat to induce recrystallization, more initial strain causes a more rapid and greater overall restoration of mechanical properties for a fixed time and temperature of anneal.

#### 4.4. Effect of annealing on hardness

Data from Table 4.7 are graphed in Fig. 4.14 with time as the abscissa and  $R_B$  hardness as the ordinate. At an annealing temperature of 100°C—shown in 4.14 (a)—the hardness values for the 0% and 25% CW specimens experience no significant changes over an entire week’s duration. The temperature is low and there is not enough initial strain. Changes in properties are mediated by thermally activated diffusion of atoms, which is driven by strain energy. For the 0% CW samples, there is no strain and thus no driving force. For the 25% CW samples, the strain energy is not enough to drive any material changes at this temperature.

On the other hand, the 50% and 75% CW specimens both show a slow decrease in hardness from 24 hours to the 1-week mark. Although these two specimens carry a lot of initial strain to drive material changes, the temperature of anneal is far too low; 100°C is below the recrystallization temperature. The microstructure of a 75% CW coupon annealed at 100°C for 30 minutes—Fig. 1 (a) in *Metallography study 1, section A.1*—exhibits residual elongation of grains due to cold work. No recrystallization or macroscopic change in grain structure is observed at the 30 minute mark. The small but significant change in hardness when these two samples (50% CW, 75% CW) are annealed for a week at 100°C may be explained by the phenomenon of recovery.

At a 300°C anneal, graphing hardness as a function of annealing time—Fig. 4.14 (b)—the 0% and 25% CW specimens again experience no significant changes in hardness. There is no plastic deformation in the 0% CW samples and the 25% CW samples do not carry enough strain to induce the process of recrystallization. The 50% and 75%

CW specimens, however, experience a more significant drop in hardness than for the 100°C anneal. The onset of this descent occurs at the 30 minute mark. Therefore, the time to reach recrystallization for the 50% and 75% CW specimens occurs at least as early as 30 minutes.

An early stage of recrystallization for the 75% CW coupon is depicted in Fig. 1 (b) in *Metallography study 1, section A.1*. The extremely fine grains indicate extensive nucleation. The black spots observed across all metallographs are taken to be lead particles. Lead is seen in the microstructure as discrete, globular particles because it is practically insoluble in the FCC copper phase.

At a 425°C anneal—Fig. 4.14 (c)—hardness does not change for the 0% CW samples. However, there is a gradual decrease in hardness for the 25% CW samples. The drop-off is most significant between 2–5 minutes. Fig. 2 (b) in *Metallography study 2, section A.2* reveals the 25% CW specimen in a late stage of recrystallization at the 60-minute mark. Compared to the 0% CW specimen in Fig. 2 (a), the average grain size of the 25% CW specimen is smaller. The smaller equiaxed grains are a product of recrystallization.

At 50% CW in Fig. 2 (c), the grain size is even finer yet. The greater amount of initial strain precipitated even

**Table 4.7** Rockwell B hardness<sup>a</sup> for variable cold deformation, time and temperature of anneal

Time	Percentage deformation				Time	Percentage deformation			
	0	25	50	75		0	25	50	75
	$R_B$	$R_B$	$R_B$	$R_B$		$R_B$	$R_B$	$R_B$	$R_B$
0m <sup>b</sup>	27.5	79.5	87.0	90.0	0m	27.5	79.5	87.0	90.0
5m	26.7	77.7	92.2	92.7	5m	27.7	75.8	85.3	72.7
30m	24.5	77.2	88.5	87.2	30m	27.3	76.3	89.5	70.2
150m	23.2	81.8	93.2	90.0	150m	27.5	72.3	76.5	60.0
24h	23.2	81.7	87.0	83.2	24h	25.7	73.0	57.8	49.3
1w	29.7	75.7	69.8	68.5	1w	27.3	75.5	57.3	45.7

m-h-w = Minutes-hours-weeks at temp.  
 $R_B$  = Rockwell B hardness number

**(a) 100°C**

Time	Percentage deformation				Time	Percentage deformation			
	0	25	50	75		0	25	50	75
	$R_B$	$R_B$	$R_B$	$R_B$		$R_B$	$R_B$	$R_B$	$R_B$
0m	27.5	79.5	87.0	90.0	0m	27.5	79.5	87.0	90.0
2m	27.2	78.5	91.7	92.6	2m	26.0	70.7	55.7	62.0
5m	24.5	66.2	57.2	58.2	5m	23.7	32.5	31.7	28.8
10m	24.7	64.3	57.0	56.5	10m	20.7	33.0	33.8	15.8
30m	27.0	49.2	52.7	47.3	30m	15.8	26.0	22.8	20.5
60m	27.0	45.0	53.7	32.5	60m	22.7	29.8	30.3	17.0

m = Minutes at temp.  
 $R_B$  = Rockwell B hardness number

**(c) 425°C**

Time	Percentage deformation				Time	Percentage deformation			
	0	25	50	75		0	25	50	75
	$R_B$	$R_B$	$R_B$	$R_B$		$R_B$	$R_B$	$R_B$	$R_B$
0m	27.5	79.5	87.0	90.0	0m	27.5	79.5	87.0	90.0
2m	27.2	78.5	91.7	92.6	2m	26.0	70.7	55.7	62.0
5m	24.5	66.2	57.2	58.2	5m	23.7	32.5	31.7	28.8
10m	24.7	64.3	57.0	56.5	10m	20.7	33.0	33.8	15.8
30m	27.0	49.2	52.7	47.3	30m	15.8	26.0	22.8	20.5
60m	27.0	45.0	53.7	32.5	60m	22.7	29.8	30.3	17.0

m = Minutes at temp.  
 $R_B$  = Rockwell B hardness number

**(d) 550°C**

<sup>a</sup> Each number on the chart represents an average hardness taken from 4 unique coupons and 3 trials for each coupons. Thus, each  $R_B$  number listed in the chart is an average of 12 measurements.

<sup>b</sup> Specimens in the 0m category are not annealed.

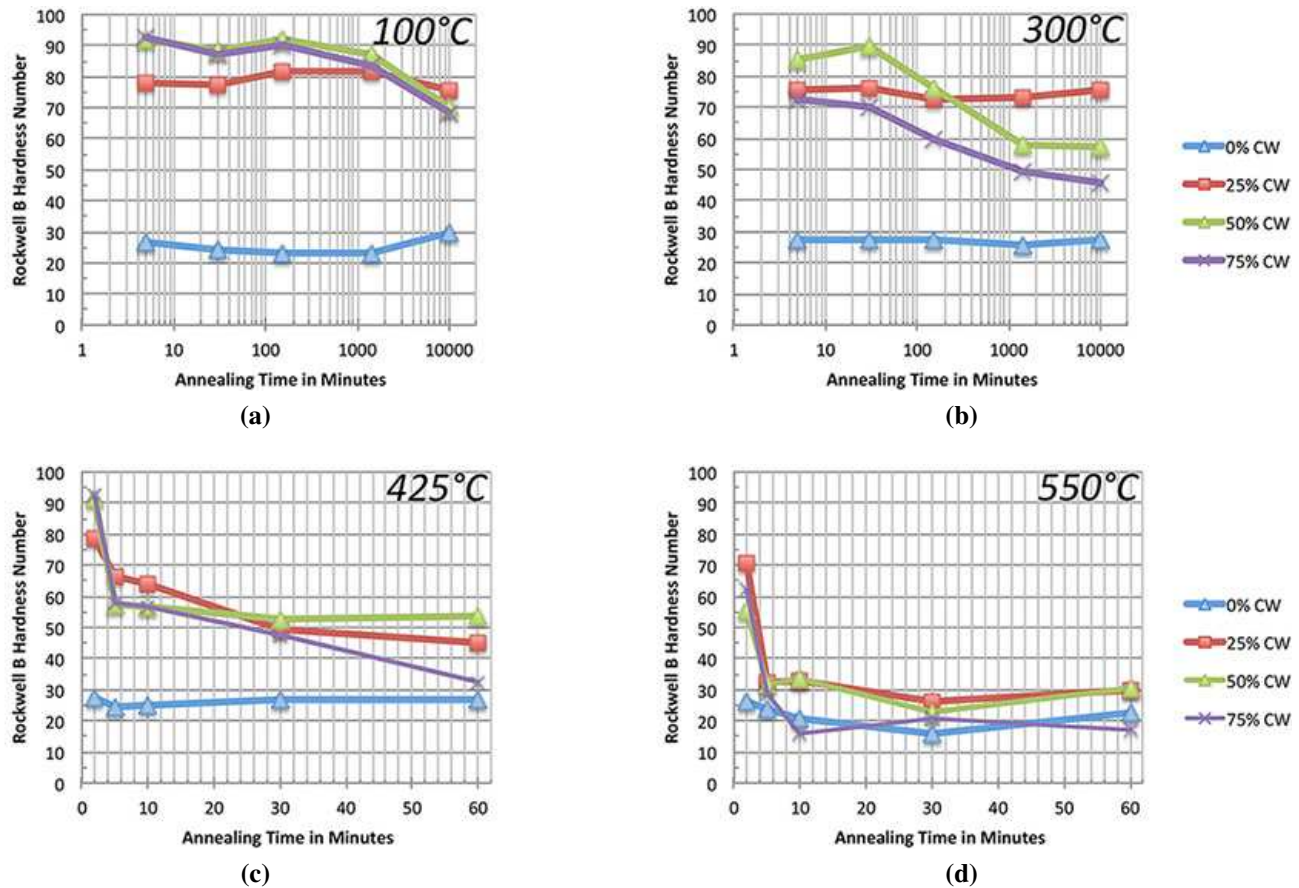


**Fig. 4.14** Hardness  $R_B$  as a function of annealing time for fixed temperatures of anneal. Data are derived from Table 4.7. For each annealing temperature there are four specimens each of different degrees of cold deformation (0%, 25%, 50%, and 75% CW). Graphs (a) and (b) have 5 distinct time intervals corresponding to annealing times of 5 min, 30 min, 150 min, 24 hr, and 1 week. The x-axis is in minutes and implements a log base 10 scale. Graphs (c) and (d) have 5 distinct time intervals corresponding to annealing times of 2 min, 5 min, 10 min, 30 min, and 60 min. The x-axis is a linear time scale in minutes. For a better depiction of the data see Fig. 4 in the Appendix section A.4.

more nucleation and hence, a smaller average grain size. Considering hardness began a steep decline at 2 minutes, by 60 minutes at a 425°C anneal recrystallization is in an advanced stage. *Tensile study 1, section 4.2* confirms that at 425°C, recrystallization began as early as 2 minutes for the 50% CW samples. Recall that Fig. 4.7, 4.8, and 4.9, show that  $\sigma_y$ ,  $\sigma_{TS}$ , and % EL begin a significant change at 2 minutes—which parallels the behavior of hardness. Hardness goes from 91.7  $R_B$  at 2 minutes to 57.2  $R_B$  at 5 minutes.

At 75% CW there is a sharp drop in hardness at least as early as 2 minutes. The decline in hardness continues even after an hour although at a slower rate. The metallography at the 60-minute mark for a 75% CW coupon at 425°C in Fig. 2 (d) demonstrates that the grain size is nearly as coarse as the 0% CW specimen. The 75% CW specimen is almost fully restored in terms of microstructure and hardness to the precold-worked state after one hour. Because of

the immense strain energy and favorable temperature, the process of recrystallization is nearly driven to completion. The graph of hardness vs. time at the greatest annealing temperature, 550°C—Fig. 4.14 (d)—shows the most precipitous drop in hardness for each of the cold-deformed coupons. As expected, the hardness of the non-deformed coupons are unaffected by annealing. Within 5 minutes, the 25% and 50% CW specimens exhibit a lower hardness number than was reached after an hour in the 425°C anneal.

*Metallography study 3, section A.3* tracks the microstructure of the 50% CW specimen from 5 minutes to 60 minutes at the 550°C annealing temperature. At a time of 5 minutes—which is shown in Fig. 3 (a)—there is a coarser grain size compared to the 60-minute mark at 425°C—shown in *Metallography study 2, section A.2* in Fig. 2 (c). In other words, the 50% CW sample is further along in the recrystallization process within 5 minutes at 550°C compared to 60 minutes at 425°C. This demonstrates the exponential

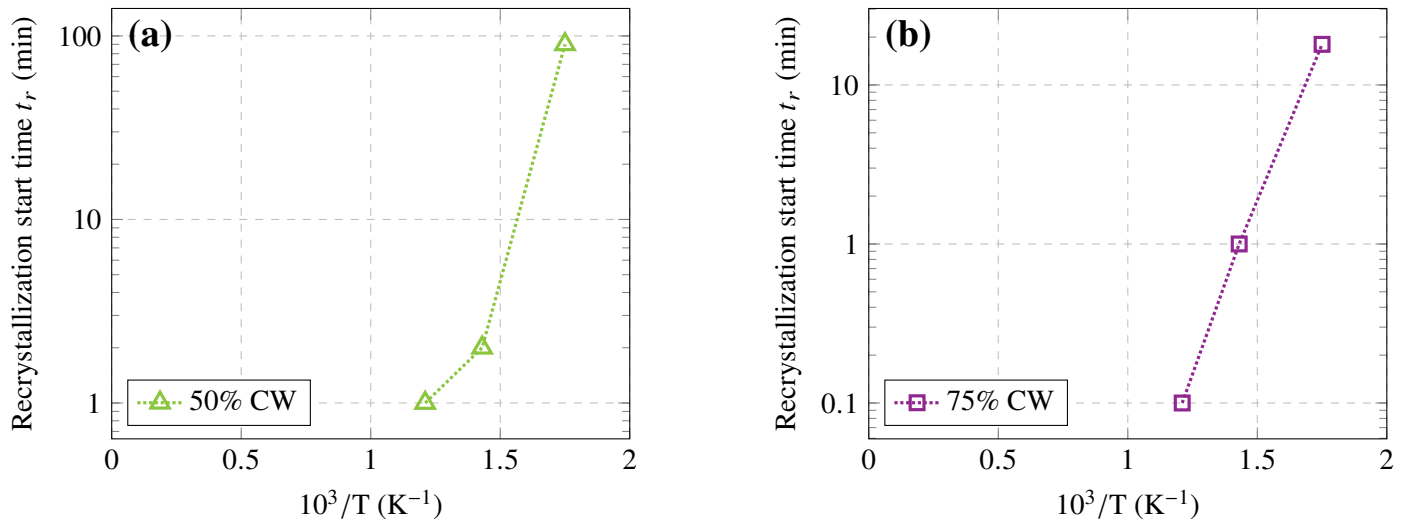


**Fig. 4.15** Time to start recrystallization vs.  $10^3/T$  for cartridge brass cold rolled to 50% and 75% CW. A log axis of  $t_r$  against the inverse of absolute temperature is employed in order to demonstrate the thermally-activated phenomenon of recrystallization.

effect of increasing temperature on atomic diffusion and the restoration processes that accompany it.

As time passes after the 5-minute mark for the 50% CW specimen, the average grain size grows coarser maintaining an equiaxed grain structure. By 60 minutes, the grain size and shape closely resemble the un-deformed 0% CW specimen—the un-deformed specimen is shown in *Metallography study 2, section A.2* Fig. 2 (a). The hardness values are comparable as well.

In *Metallography study 1, section A.1* Fig. 1 (d), the 75% CW coupon microstructure is shown at 30 minutes time and 550°C annealing temperature. This is the coarsest microstructure observed yet. The high temperature and immense strain energy drives recrystallization to rapid completion. Appreciable grain growth has occurred by the 30-minute mark.

#### 4.5. Dependence of recrystallization on anneal time, temperature, and cold work

Fig. 4.15 (a) and (b) plot the time to reach the start of recrystallization against the inverse of the absolute temperature for 50% CW and 75% CW, respectively. When a logarithmic base 10 scale is used for the time to reach recrystallization, the curve assumes a linear shape. This reinforces the exponential effect of increasing temperature on how rapidly recrystallization occurs. For a given degree of cold deformation, as the temperature is increased, the time it takes to reach the start of recrystallization goes down exponentially.

Based off the hardness data, the times to reach recrystallization  $t_r$  for a given annealing temperature are estimated in Table 4.8. The 0% CW sample did not recrystallize and thus, is not tabulated. The times shown are extremely

crude approximations. The major difference is in the extent to which recrystallization occurs at a given temperature, which is a function of % CW. In order to more accurately predict times to recrystallization at a given temperature, more data is needed at more time intervals.

Based off *Tensile study 2, section 4.3*, the recrystallization temperature for the 75% CW specimen was determined to be between 300°C and 425°C for a time of anneal of 5 minutes. Looking at *Metallography study 1, section A.1* Fig. 1 (b) at 300°C at the 30-minute mark there is significant recrystallization underway. Based off the hardness data—Fig. 4.14 (b)—a gradual drop in hardness is detected at 5 minutes onwards to a week. Therefore, it is safe to assume that at a 300°C anneal, the 75% CW specimen begins recrystallizing by 30 minutes at the latest but may occur as early as 5 minutes.

**Table 4.8** Approximate time to reach recrystallization

Temperature	Recrystallization start time, $t_r$	Temperature	Recrystallization start time, $t_r$
550°C	2 min	550°C	< 2 min
425°C	2–5 min	425°C	2 min
300°C	No recrystallization	300°C	30–150 min
100°C	No recrystallization	100°C	No recrystallization

(a) 25% CW

(b) 50% CW

Temperature	Recrystallization start time, $t_r$
550°C	instantaneous
425°C	< 2 min
300°C	5–30 min
100°C	No recrystallization

(c) 75% CW

## V. CONCLUSION

The exact recrystallization temperature for the annealing times of 5 and 30 minutes is less definitive in the case of the 50% CW specimen. Fig. 2 (c) in *Metallography study 2, section A.2* shows a fine grain microstructure in the 50% CW sample after 60 minutes of annealing at 425°C. This is in contrast to the 0% CW specimen, which is much coarser.

For 50% CW annealed at 425°C, there is a significant drop in hardness first detected between 2 and 5 minutes—Fig. 4.14 (c). Based on the tensile data in *Tensile study 1, section 4.2*, for an annealing temperature of 425°C, recrystallization begins at a time of anneal of approximately 2 minutes. With this in mind, it is with more certainty that for the 50% CW cartridge brass specimens  $T_r = 425^\circ\text{C}$  for an annealing time of 2 minutes.

At an even greater annealing time of 30 minutes, the recrystallization temperature for 50% CW brass specimens is likely to be 300°C. Hardness —Fig. 4.14 (b)—begins a drop-off at the 30 minute mark. This is a rough estimate. Additional metallographic and tensile data at 50% CW and annealing at 300°C should be gathered to confirm  $T_r = 300^\circ\text{C}$  for a 30 minute anneal.

For an increase in cold deformation there is an observed effect on the mechanical properties where  $\sigma_y$  and hardness respond most dramatically. The marginal change in mechanical properties ( $\sigma_y$ ,  $\sigma_{TS}$ , and % EL,  $R_B$ ) decreases for each marginal increase in cold deformation. Thus, at the early stages of cold work there are more significant alterations in mechanical properties.

Tensile tests, hardness data, and metallographic examination serve as three independent methods to pinpoint the time to reach recrystallization  $t_r$  for a fixed annealing temperature and degree of deformation and the recrystallization temperature  $T_r$  for a fixed annealing time and degree of deformation. For instance, based on the drop in yield and ultimate strengths from the tensile test, a  $T_r = 300$  to 425°C was predicted for 75% CW specimens annealed for 5 minutes. Hardness data showed a marked decrease starting as early as 5 minutes. Metallographic examination for the 75% CW coupon annealed for a time of 30 minutes showed clear evidence of recrystallization. Therefore, a recrystallization temperature of  $T_r = 300^\circ\text{C}$  was defined as having an annealing time between 5 and 30 minutes for the 75% CW specimen.

Temperature has an exponential effect on the time to reach recrystallization. Increased temperature greatly enhanced the rate and intensity at which mechanical properties were restored. Similar to the effect of temperature, increasing the degree of cold deformation enhances the tendency to return to the precold-worked state. The driving force of the raised free energy enhances the rate of recrystallization and effectively lowers the heat requirement needed to induce recrystallization.

## REFERENCES

1. H. L. Walker. "Grain Sizes Produced by Recrystallization and Coalescence in Cold-rolled Cartridge Brass," *Eng. Exp. Station*, 1945, vol. 43, p. 7.
2. M. C. Lovell, A. J. Avery, and M. W. Vernon, "Mechanical Properties of Materials," in: *Physical Properties of Materials*, Springer Netherlands, 1976, pp. 87–105.
3. M. D. Bever, D. I. Holt, and A. I. Titchener, "The Stored Energy of Cold Work," *Prog. in Mat. Sci.* 1973, vol. 17, pp. 5–177.
4. R. Abbaschian, R. E. Reed-Hill, "Stored Energy of Cold Work," in: *Physical Metallurgy Principles*, Third edition, PWS-Kent Publishing, Boston, MA, 1991, pp. 227–28.
5. B. Devincere, T. Hoc, and L. Kubin, "Dislocation Mean Free Paths and Strain Hardening of Crystals," *Science*, 2008, vol. 320, pp. 1745–748.
6. W. D. Callister, "Mechanisms of Strengthening in Metals," in: *Materials Science and Engineering: An Introduction*, Eighth edition, John Wiley and Sons, New York, NY, 2007, pp. 211–18.
7. P. L. Mangonon, "Plastic Deformation and Annealing," in: *The Principles of Materials Selection for Engineering Design*, US edition, Prentice Hall, Upper Saddle River, NJ, 1999, pp. 270–315.
8. I. Baker, "Recovery, Recrystallization, and Grain Growth in Ordered Alloys," *Intermetallics*, 2000, vol. 8, pp. 1183–96.
9. R. E. Reed-Hill, "Annealing," *Physical Metallurgy Principles*, First edition, Van Nostrand, Princeton, NJ, 1964, pp. 227–71.
10. E. Mittenmeijer, "Recovery" in: *Fundamentals of Materials Science: The Microstructure-property Relationship—Using Metals as Model Systems*, First edition, Springer, New York, NY, 2010, pp. 463–70.
11. R. W. Cahn, "Recovery and Recrystallization," in: *Physical Metallurgy*, Fifth edition, (D. E. Laughlin and K. Hono, eds.), Elsevier, 2014, pp. 2291–2397.
12. R. W. Cahn, "Recovery and Recrystallization," in: *Physical Metallurgy*, Third edition, (R. W. Cahn and P. Haasen, eds.), North-Holland Physics Publishing, Amsterdam, 1983, pp. 1593–1611.
13. M. F. Mehl, "Recrystallization," in: *Metals Handbook*, First edition, American Society for Metals, Cleveland, OH, 1948, pp. 259–263.
14. J. E. Burke and D. Turnbull, "Recrystallization and Grain Growth," *Prog. in Met. Phy.* 1952, vol. 3, pp. 220–92.
15. F. J. Humphreys and M. Hatherly, "The Laws of Recrystallization," in: *Recrystallization and Related Annealing Phenomena*, First edition, Pergamon, Oxford, UK, 1995, pp. 177–78.
16. Q. Guo-Zheng, "Characterization for Dynamic Recrystallization Kinetics Based on Stress-Strain Curves," in: *Recent Developments in the Study of Recrystallization*, (P. Wilson, ed.), 2013, pp. 61–88.
17. A. Rollett, F. J. Humphreys, G. S. Rohrer, and M. Hatherly, "The Formal Kinetics of Primary Recrystallization," in: *Recrystallization and Related Annealing Phenomena*, Second edition, Elsevier, 2004, pp. 232–9.
18. Y. Fukuda, Y. Kado, T. Yoshikawa, and K. Oishi, Y. Mae, "Diffusion Distances of the Constituent Atoms in the Metallurgical Phenomena Such as Recovery, Recrystallization, Grain Growth, and Aging in Aluminum and Copper Alloys," *J. of Mat. Eng. and Perform.* 2002, vol. 11, pp. 544–50.
19. "Cartridge Brass UNS C26000," *AZOM: Material Information*, 2015.
20. E. Mittenmeijer, "Grain Growth," in: *Fundamentals of Materials Science: The Microstructure-property Relationship*, First edition, Springer, New York, NY, 2010, pp. 477–96.
21. F. C. Campbell (ed.), "Recovery, Recrystallization, and Grain Growth," in: *Elements of Metallurgy and Engineering Alloys*, First edition, Materials Park, OH, ASM International, 2008, pp. 117–33.
22. B. Kim, K. Hiraga, and K. Morita, "Kinetics of Normal Grain Growth Depending on the Size Distribution of Small Grains," *Mat. Trans.* 2004, vol. 44, pp. 2239–44.
23. J. E. Burke, "Some Factors Affecting the Rate of Grain Growth in Metals (70:30 Brass)," *Trans. of the AIME* 1949, vol. 180, pp. 73–91.
24. M. A. Fortes, "Grain Growth Kinetics: The Grain Growth Exponent," *Mat. Sci. Forum*, 1992, vols. 94-96, pp. 319–24.
25. H. Conrad, "Effect of Grain Size on the Lower Yield and Flow Stress of Iron and Steel," *Acta Met.* 1963, vol. 11, pp. 75–77.

26. L. E. Gibbs, *Cold Working of Brass: With Special Reference to Cartridge (70-30) Brass*, First edition, American Society for Metals, Cleveland, OH, 1946, p. 10.
27. A. A. Gorni, "Spreadsheet Applications in Materials Science," in: *Spreadsheets in Science and Engineering*, (G. Filbe, ed.), First edition, Springer-Verlag Berlin Heidelberg, 1998, pp. 229-60.
28. ASTM, "Standard Classification for Temper Designations for Copper and Copper Alloys—Wrought and Cast, B 601," in: *Annual Book of ASTM Standards*, ASTM International, Philadelphia, PA, 2011, pp. 1–5.
29. "Cartridge Brass, UNC C26000 (260 Brass) OS Temper," *MatWeb: Material Property Data*, 2015.
30. "Cartridge Brass, UNC C26000 (260 Brass) H Temper," *MatWeb: Material Property Data*, 2015.
31. T. B. Massalski (ed.), *Binary Alloy Phase Diagrams*, Second edition, vol. 2, American Society for Metals, Metals Park, OH, 1990.
32. C. Gilmore, "Annealing Metals," in: *Materials Science and Engineering Properties*, First edition, Cengage Learning, Boston, MA, 2014, pp. 325–6.
33. H. L. Walker. "Grain Sizes Produced by Recrystallization and Coalescence in Cold-rolled Cartridge Brass," *Eng. Exp. Station*, 1945, vol. 43, pp. 5–69.
34. ASTM, "Standard Test for Tension Testing of Metallic Materials, E8—6, Test Specimens" in: *Annual Book of ASTM Standards*, ASTM International, Philadelphia, PA, 2011, pp. 2–10.
35. ASTM, "Standard Test for Tension Testing of Metallic Materials, E8—5, Apparatus" in: *Annual Book of ASTM Standards*, ASTM International, Philadelphia, PA, 2011, p. 2.

## A. APPENDIX

### A.1. Metallography study 1 – annealing temperature

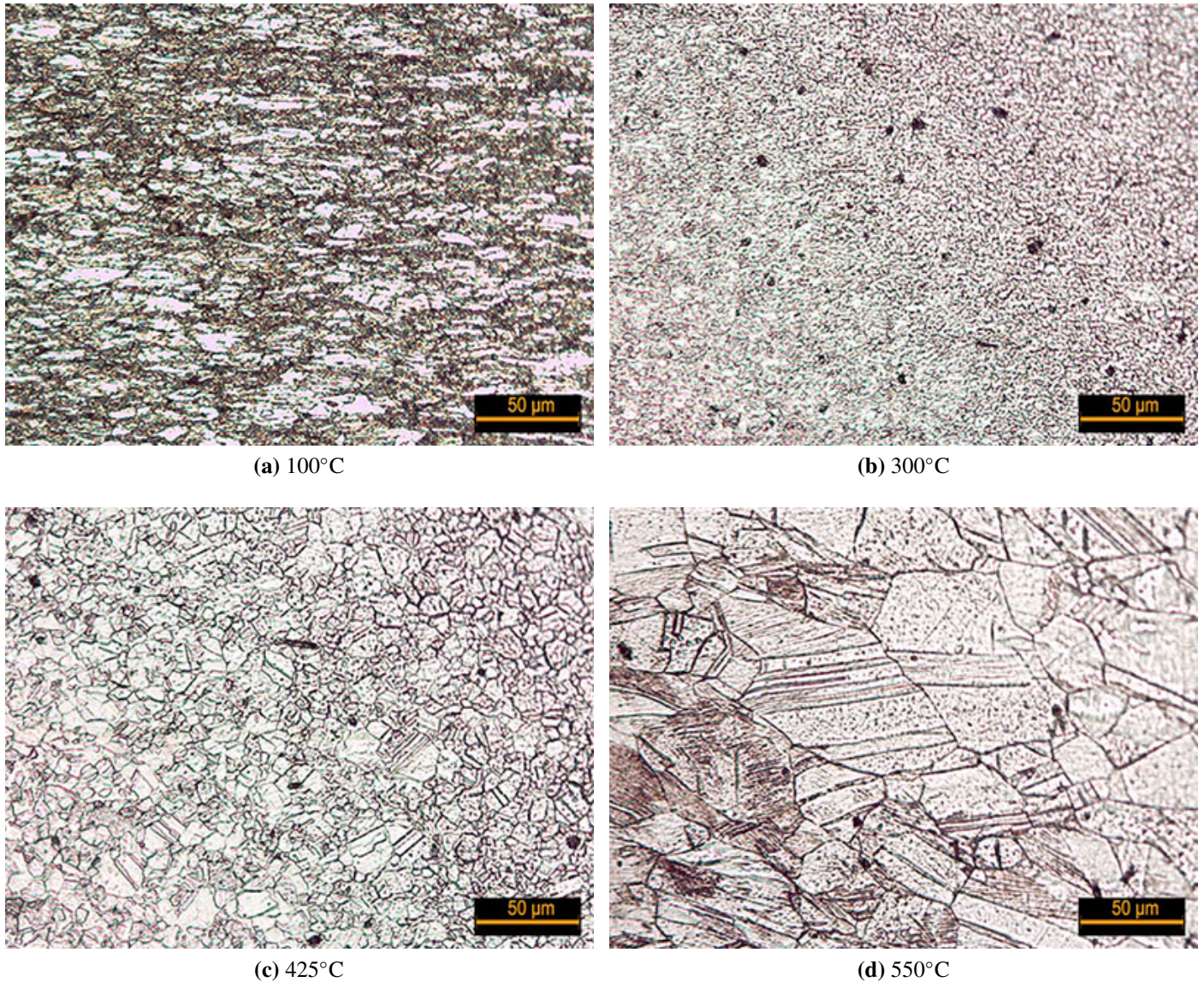


**Fig. 1** Microstructure of cartridge brass cold rolled to 75% CW and annealed for 30 min at four different annealing temperatures. Images are at 200X magnification.

#### Comments:

(a): Resembles the cold-worked state with highly elongated grains. The increase in grain boundary area is a mechanism by which cold work increases the stored energy of the material. No recrystallization has occurred yet.

(b): Towards the onset of recrystallization. Time to recrystallization is no later than 30 minutes. The high degree of plastic deformation (75% CW) is the driving factor for the nucleation of extremely fine grains. Hardness has already started to decline as of 5 minutes. While definitely in the early stages of recrystallization, this may not be the very beginning.

(c): Undergoing high-angle grain boundary migration and at a more advanced stage of recrystallization relative to (b). Hardness has already experienced large decreases within the first 5 to 10 minutes. Further decreases in hardness will not be as pronounced.

(d): Completed recrystallization and already undergone appreciable grain growth. Hardness is now below the precold-worked state.

## A.2. Metallography study 2 – cold work

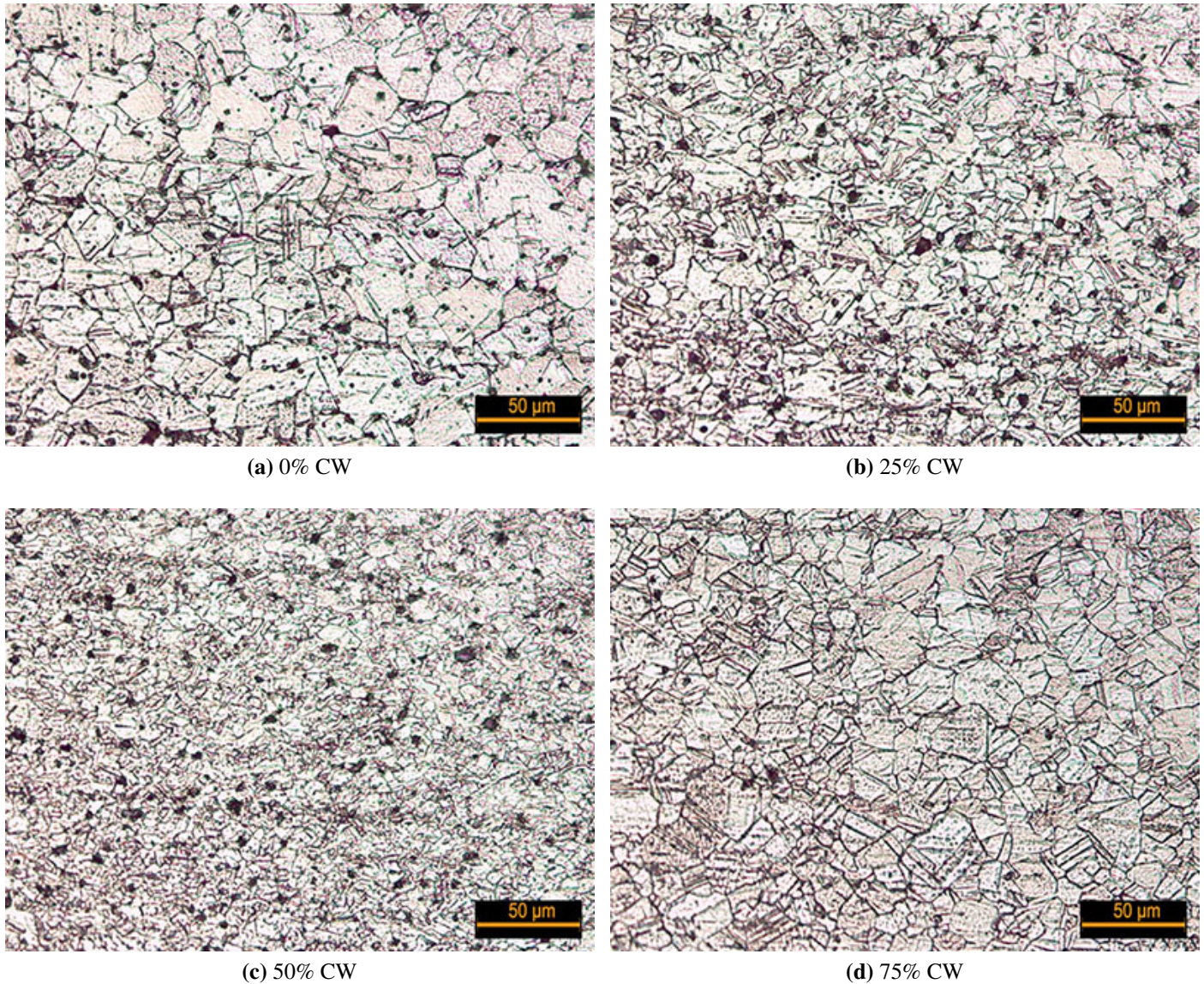


**Fig. 2** Microstructure of cartridge brass annealed for *60 min* at *425°C* under four different levels of cold work. Images are at 200X magnification.

Comments:

(a): Undeformed brass (not cold rolled). There are no significant changes in grain structure nor changes in hardness because there is no initial strain energy.

(b): Well into the process of recrystallization by 60 minutes. Hardness has already dropped significantly. With less cold deformation (25% CW) the average grain size is larger relative to high degrees of cold deformation.

(c): Recrystallization already started and undergoing high-angle grain boundary migration. The average grain size is smaller than the 25% CW specimen in Fig. (b) because of greater amounts of nucleation. Hardness is slightly greater than (b) right now. However, hardness already dropped precipitously within the first 5 minutes at this temperature.

(d): Resembles the undeformed (0% CW) state meaning that the process of recrystallization has almost completely restored the metal to the fully annealed/precold-worked state. The hardness is slightly higher than 0% CW and the grain size on average appears to be slightly smaller.

### A.3. Metallography study 3 – annealing time

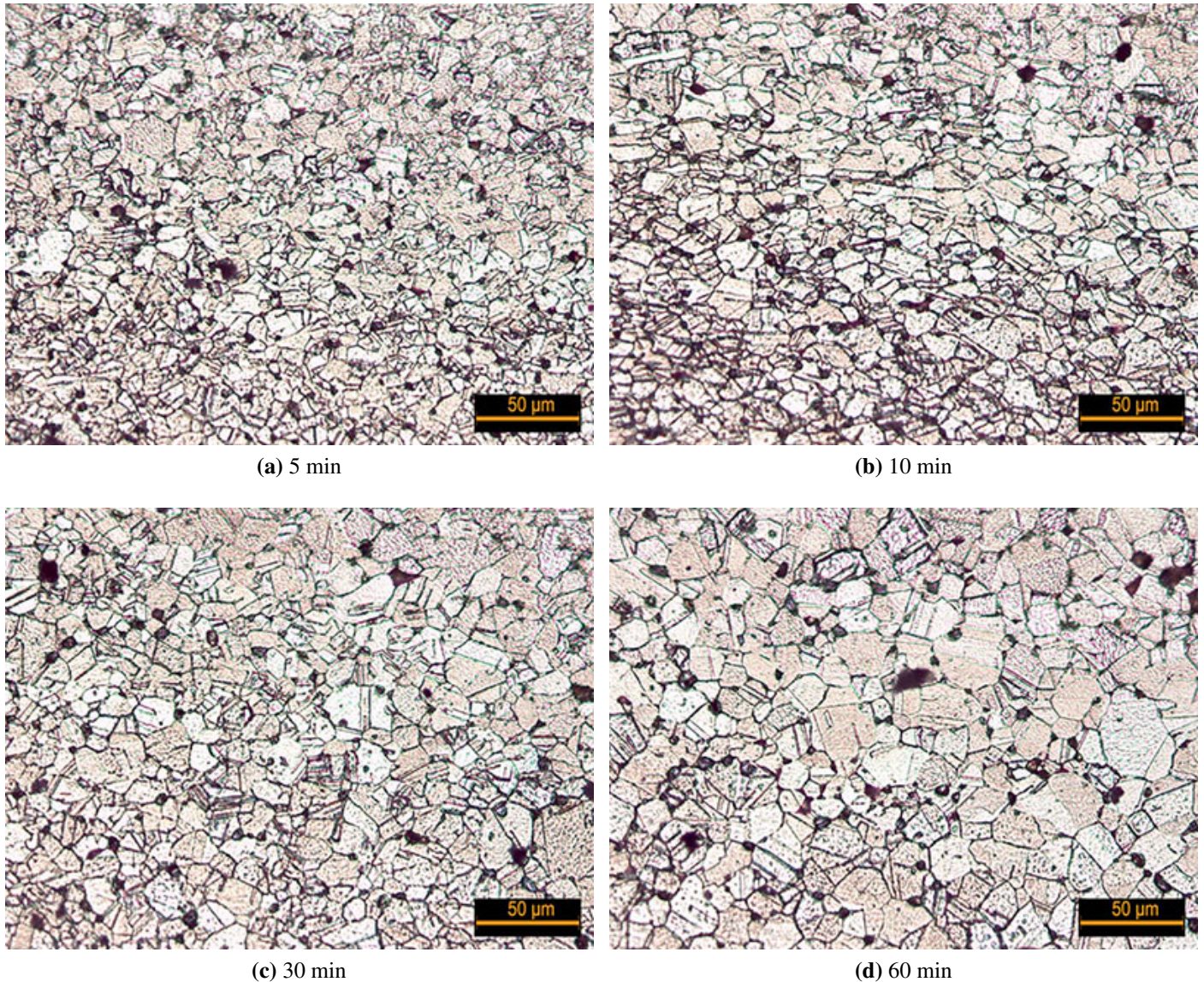


**Fig. 3** Microstructure of cartridge brass cold rolled to *50% CW* and annealed at *550°C* for variable time. Images are at 200X magnification.

Comments:

(a): Recrystallization already begun and undergoing high-angle grain boundary migration.

(b): Larger grains grow at the expense of smaller grains and there is further decreases in hardness.

(c): same as (b), more grain boundary migration occurs.

(d): Resembles the undeformed (*0% CW*) state meaning that the process of recrystallization has almost completely restored the metal to the fully annealed/precold-worked state. Grains are larger and maintain the equiaxed state.

Unfortunately, this set of metallographic data is not as exciting. At such a high temperature, all the interesting recrystallization events occurred at times less than 5 minutes. Nevertheless, the details of the restoration process at the advanced stages of recrystallization are still worth seeing step by step.

#### A.4. 3D surface (time, % CW, hardness)

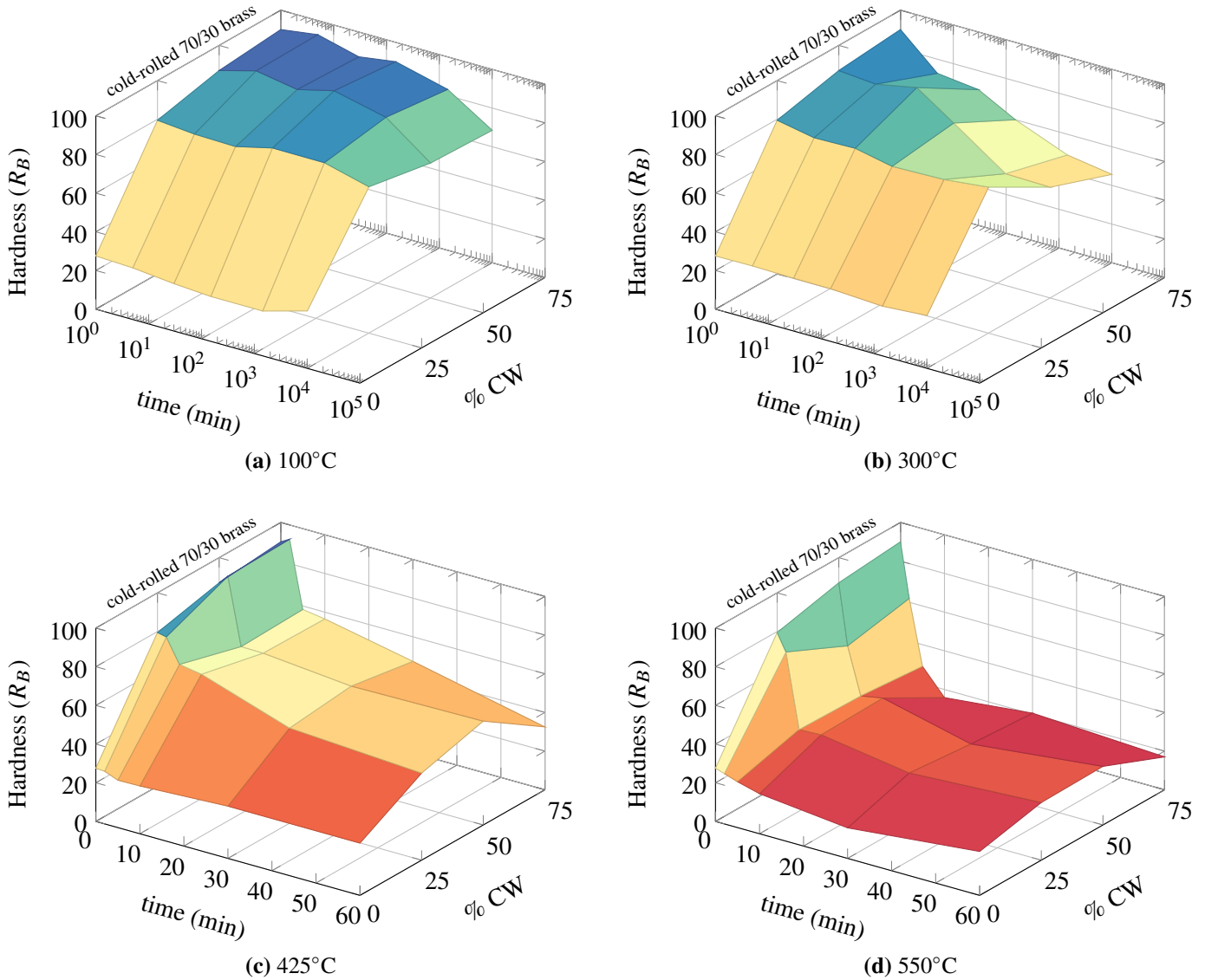


**Fig. 4** Hardness as a function of a time and % CW at the four annealing temperatures. The 3D plots are data from Table 4.7. These 3D plots are projected in Fig. 4.14. Three dimensional renderings of the data more emphatically demonstrate the effect of temperature on hardness. At 100 and 300°C a log time axis is developed. The strained specimens (25, 50, and 75% CW) do not see dramatic changes in hardness over a week's period. The temperature is too low to induce recrystallization despite the initial strain energy. Using a linear time scale at 425 and 550°C temperatures, hardness drops off rapidly at least as early as 2 minutes. The effect is most pronounced at 550°C.